

DOCKETED	
Docket Stamp Updated:	2/8/2022 2:12:40 PM
Docket Number:	19-SPPE-04
Project Title:	SJ2
TN #:	241479
Document Title:	Ada E Márquez Comments on CEQA Comment Letter Appendix A Ref (6 of 8)
Description:	Due to docket staff error, the document was docketed on February 7, 2022, not February 8, 2022.
Filer:	System
Organization:	Ada E. Márquez
Submitter Role:	Public
Submission Date:	2/8/2022 12:00:43 PM
Docketed Date:	2/7/2021

DOCKETED	
Docket Number:	19-SPPE-04
Project Title:	SJ2
TN #:	241479
Document Title:	Ada E Márquez Comments on CEQA Comment Letter Appendix A Ref (6 of 8)
Description:	N/A
Filer:	System
Organization:	Ada E. Márquez
Submitter Role:	Public
Submission Date:	2/8/2022 11:11:08 AM
Docketed Date:	2/8/2022

Comment Received From: Ada E. MÃ¡rquez
Submitted On: 2/8/2022
Docket Number: 19-SPPE-04

**Ada E MÃ¡rquez Comments - CEQA Comment Letter Appendix A
Ref (6 of 8)**

Additional submitted attachment is included below.

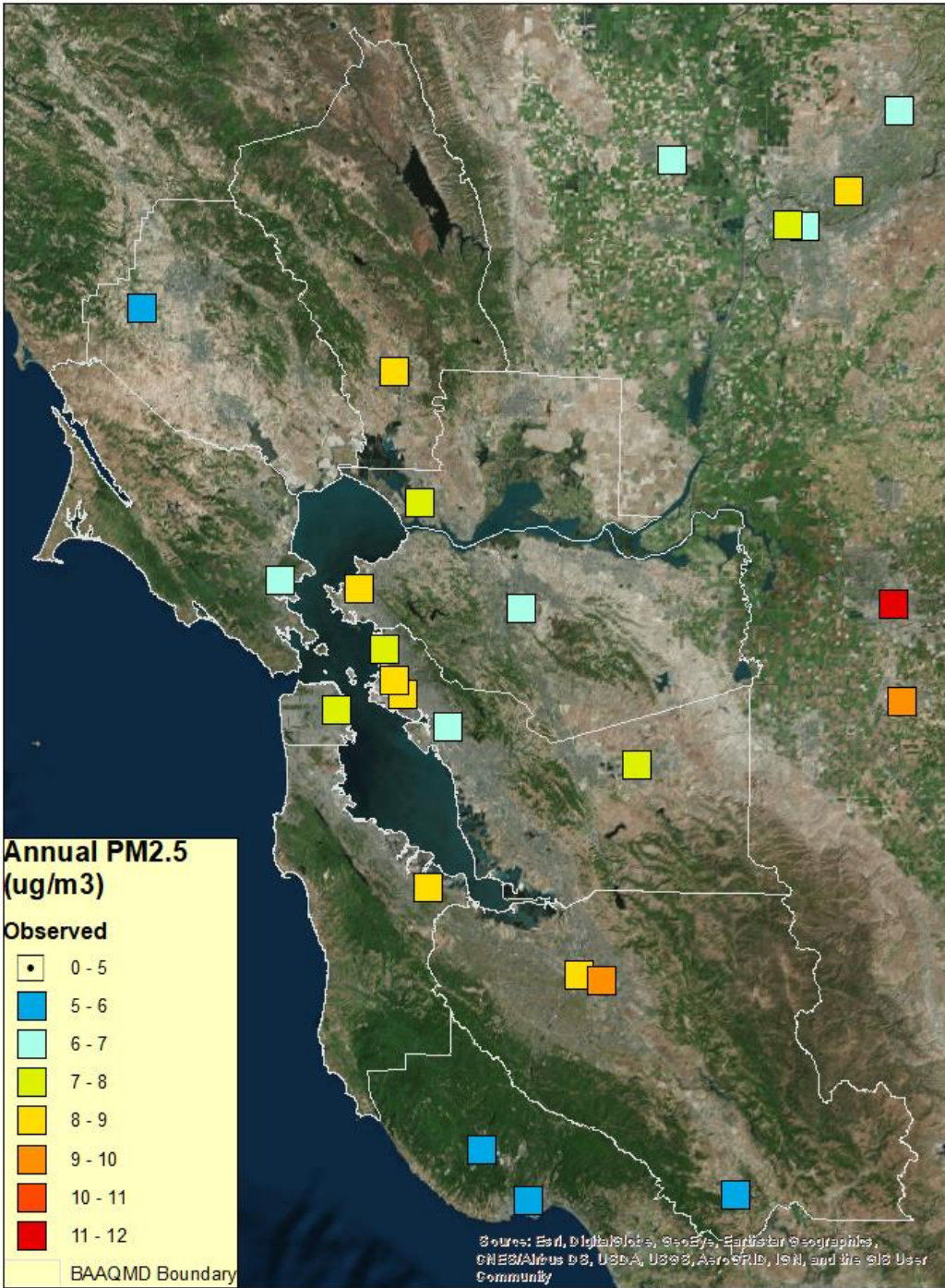


Figure 2.1: Spatial distribution of observed annual average PM_{2.5} concentrations for 2016 within the 1-km modeling domain.

3. Modeling

3.1 Emissions Inventory Preparation

The 2016 modeling emissions inventory includes estimates for area sources,² point sources, onroad mobile sources, nonroad mobile sources, and biogenic sources. The inventory was assembled from a variety of data sources, including the District's in-house emissions estimates, emissions data from ARB, and outputs from ARB's EMFAC2017 model (see Table 3.1). ARB emissions data were used for all anthropogenic sources in non-BAAQMD counties with the exception of onroad mobile sources. County- and facility-level ARB emissions data for the entire state of California were downloaded from ARB's FTP site in June 2018. These data were in SMOKE-ready format and were consistent with the current version of ARB's online repository of emissions inventory data that was developed to support the preparation of ozone State Implementation Plans (SIPs) for non-attainment areas in California. At the time of this work, the latest version of ARB's SIP inventory was version 1.05, which was prepared for a base year of 2012 and projected to various future years, including 2016.³

For area sources, ARB's county-level emissions estimates for residential wood combustion in BAAQMD counties were adjusted to account for the impact of the District's winter Spare the Air program, which prohibits wood burning when air quality is forecast to be unhealthy. This adjustment was based on survey-based wood combustion emissions estimates developed by District staff, comparisons with wood combustion emissions estimates for other air districts, and discussions with ARB staff. Additional details in residential wood combustion emissions are provided in Appendix B.

For onroad mobile sources, ARB's EMFAC2017 model was run for the entire state of California for each month in 2016 to produce county-level, month-specific emissions estimates. EMFAC2017 reports emissions by vehicle type and emission mode (e.g., idling, running exhaust, brake wear, tire wear). EMFAC2017 outputs were converted to SMOKE-ready format using a Perl script developed by BAAQMD staff.

For point sources, ARB emissions estimates for BAAQMD counties were replaced by detailed, in-house data prepared in California Emission Inventory Development and Reporting System (CEIDARS) format. These point source emissions data were representative of calendar year 2012 and were projected to 2016 using industry-specific growth factors from ARB's California Emissions Projection Analysis Model (CEPAM). The CEIDARS data were converted to SMOKE-ready format using a Perl script developed by BAAQMD staff.

Biogenic emissions estimates were prepared using EPA's Biogenic Emission Inventory System (BEIS), version 3.61, which estimates emissions from vegetation and soil using land use data;

² Area sources are stationary sources such as dry cleaners that are too small or numerous to treat as individual point sources.

³ See <http://www.arb.ca.gov/app/emsinv/2016ozsip/2016ozsip/>.

vegetation-specific emission rates for isoprene and other species; and gridded, hourly meteorological data from the WRF model.

3.1.1 SMOKE Processing

Emissions inventory data assembled from the sources described above were processed through version 4.5 of the SMOKE emissions processor to develop CMAQ-ready emissions inputs for each day of 2016. SMOKE uses the processing steps described below to convert “raw” emissions inputs to the spatial, temporal, and chemical resolution required by CMAQ or an equivalent air quality model.

Table 3.1: Summary of data sources used to develop the 2016 modeling inventories.

Region	Source Sector	Data Source
BAAQMD Counties ^a	Area	ARB county-level emissions estimates, with adjustments made to residential wood combustion emissions
	Nonroad	ARB county-level emissions estimates
	Onroad	County-level, month-specific EMFAC2017 outputs
	Point	In-house CEIDARS data
	Biogenic	Hourly outputs from EPA’s BEISv3.61 model
Non-BAAQMD Counties	Area	ARB county-level emissions estimates
	Nonroad	ARB county-level emissions estimates
	Onroad	County-level, month-specific EMFAC2017 outputs
	Point	ARB facility-level emissions estimates
	Biogenic	Hourly outputs from EPA’s BEISv3.61 model

^aAlameda, Contra Costa, Marin, Napa, San Francisco, San Mateo, and Santa Clara counties, plus the southern portion of Sonoma County and the western portion of Solano County.

Spatial allocation

SMOKE assigns county- or facility-level emissions to individual grid cells in the modeling domain. For point sources, emissions are assigned to grid cells based on the location coordinates (i.e., latitude and longitude) of emission release points. For county-level area, nonroad, or onroad emissions estimates, SMOKE allocates emissions to grid cells using spatial allocation factors developed from “surrogate” geospatial data sets such as land use or socioeconomic data. Geospatial data sets used to develop the surrogates used in SMOKE include land use data from the Association of Bay Area Governments (ABAG) (Reid, 2008). For counties in the District’s jurisdiction, gridded surrogate data were available at 1-km grid resolution. However, for counties outside the District, only 4-km surrogate data were available, so these data were parsed to create a set of pseudo 1-km surrogates.

Temporal allocation

SMOKE assigns annualized or average day emissions to the specific dates and hours being modeled using temporal profiles that reflect source-specific activity patterns by month, day of week, and hour of day. Temporal profiles from ARB’s CEIDARS database were used in SMOKE to

temporally allocate area, point, and nonroad mobile source emissions. For onroad mobile sources, temporal profiles that ARB developed from its California Air Resources Board Vehicle Activity Database (CalVAD) were used.⁴

Chemical speciation

SMOKE disaggregates total organic gas (TOG) and PM_{2.5} emissions into a series of model species that CMAQ uses to represent atmospheric chemistry. For the 2016 CMAQ modeling, speciation profiles developed for the SAPRC07 chemical mechanism were applied to TOG emissions from all sources, and profiles developed for the AERO6 aerosol module were applied to PM_{2.5} emissions from all sources.

The SMOKE system includes an implementation of EPA's Biogenic Emission Inventory System (BEIS), version 3.61, which estimates biogenic emissions using land use data; vegetation specific emission rates for isoprene and other species; and gridded, hourly meteorological data from the WRF model. BEISv3.61 was run within SMOKE to prepare 2016 biogenic emissions estimates for the 1-km modeling domain.

Once SMOKE runs were completed, a number of quality assurance checks were performed on the resulting emissions data. First, plots of gridded emissions were generated to examine the spatial distribution of emissions. Similarly, diurnal plots were generated to examine hourly variations in emissions by source sector and to ensure that the patterns make sense. In addition, SMOKE's SMKREPORT utility was used to generate tabular summaries of emissions by pollutant, county, grid cell, hour, and source category. This information was used in a variety of ways, including:

- Comparing emissions before and after key processing steps to ensure that any changes in the mass of emissions make sense. For example, for counties that only partially lie within the modeling domain, total emissions should decrease after the gridding step.
- Sorting emissions by source category code (SCC) or facility ID to identify key contributors to total emissions for each pollutant and to identify potential outliers.
- Summarizing emissions by pollutant and county to ensure that geographic distributions make sense (e.g., SO₂ emissions are highest in Contra Costa County where refineries are concentrated).
- Extracting emissions for grid cells in the West Oakland AERMOD modeling domain to identify key sources and compare emissions by source sector with the District as a whole.

These checks identified several issues, including PM_{2.5} hotspots at two landfills in eastern Alameda County. Our modelers worked with staff from the District's Emissions & Community Exposure Assessment section to correct the emissions from these and other point sources.

⁴ The CalVAD database fuses available data sources such as Caltrans Weigh-in-Motion (WIM) data and Highway Performance Monitoring System (HPMS) data to produce a best estimate of vehicle activity by class.

3.1.2 Emissions Summaries

This subsection provides emissions density plots and summary tables for PM_{2.5}, and similar information for additional pollutants can be found in Appendix B. Figure 3.1 shows annual average PM_{2.5} emissions for the 1-km modeling domain. Table 3.2 summarizes the annual average PM_{2.5} emissions by county and source sector, as reported by the SMOKE emissions model. Within the District's jurisdiction, annual average PM_{2.5} emissions total 33.7 tons per day (tpd). The area source sector accounts for about half of this total (17 tpd), and individual source categories that are key contributors to total PM_{2.5} emissions include residential wood combustion, fugitive dust from roadways and construction sites, and commercial cooking.

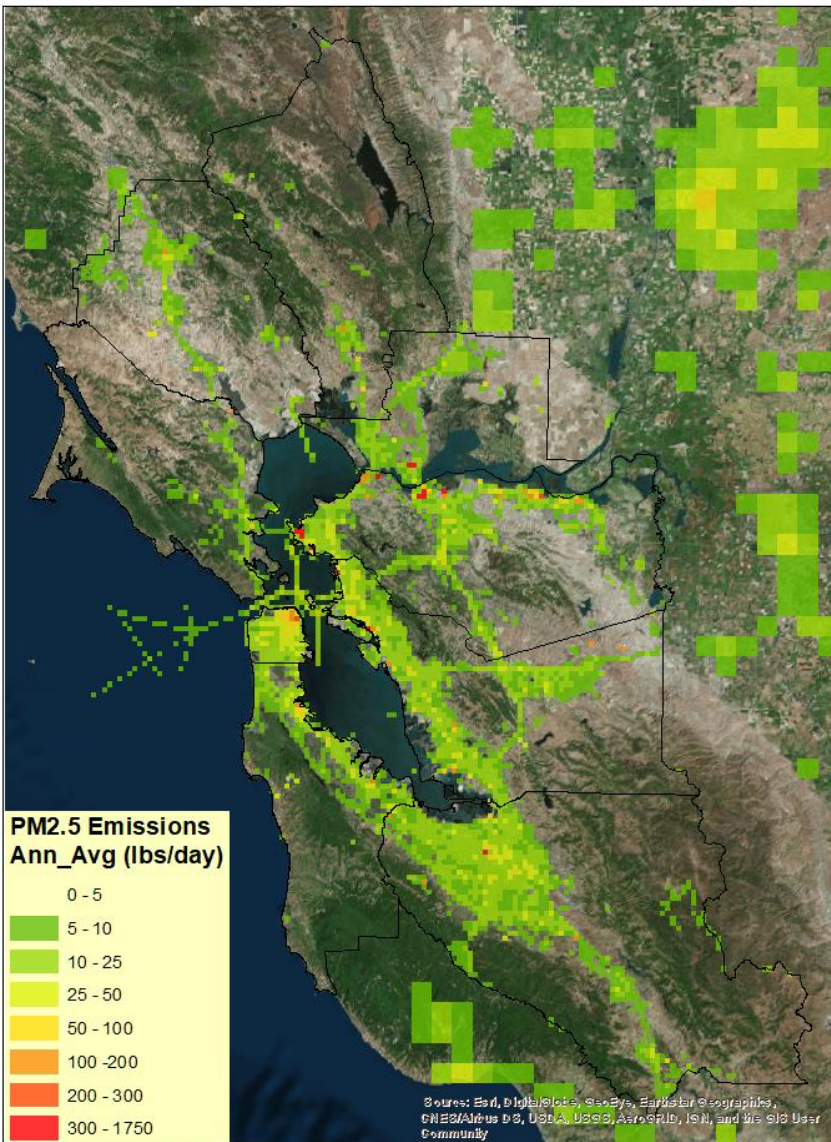


Figure 3.1: Spatial distribution of annual average PM_{2.5} emissions for the 1-km modeling domain.

Table 3.2: Summary of 2016 PM_{2.5} anthropogenic emissions (tpd) by geographic area and source sector.

Geographic Area	Area	Nonroad	Onroad	Point	Total
Alameda	3.0	0.5	1.4	1.3	6.2
Contra Costa	3.1	0.5	0.8	4.2	8.7
Marin	0.8	0.2	0.2	0.1	1.3
Napa	0.8	0.2	0.1	0.1	1.2
San Francisco	1.2	1.0	0.3	0.1	2.7
San Mateo	1.4	0.5	0.5	0.4	2.7
Santa Clara	3.9	0.6	1.3	0.7	6.5
Solano ^a	1.3	0.1	0.3	0.5	2.1
Sonoma ^a	1.4	0.3	0.3	0.2	2.2
<i>BAAQMD Subtotal</i>	<i>17.0</i>	<i>3.9</i>	<i>5.2</i>	<i>7.5</i>	<i>33.7</i>
Non-BAAQMD Counties	23.7	2.2	2.9	2.4	31.2
Domain Total	40.7	6.1	8.0	9.9	64.9

^aEmissions totals for Solano and Sonoma counties only include the portion of those counties in BAAQMD's jurisdiction.

For the West Oakland AERMOD modeling domain, annual average PM_{2.5} emissions total 0.35 tpd, or about 1% of the BAAQMD total. Figure 3.2 shows that the distribution of emissions by source sector in West Oakland differs from the District as a whole. In West Oakland, onroad and nonroad mobile sources account for 66% of total PM_{2.5} emissions, while the same sources only account for 27% of total PM_{2.5} emissions districtwide. Figure 3.3 shows the spatial distribution of PM_{2.5} emissions across the 1-km grid cells that coincide with the local-scale AERMOD modeling domain.

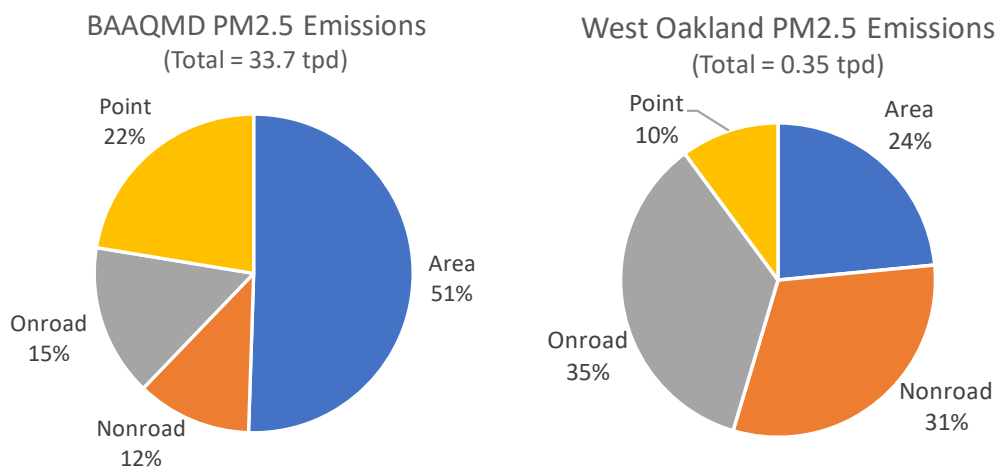


Figure 3.2: PM_{2.5} emissions by source sector for the District (left) and West Oakland (right).

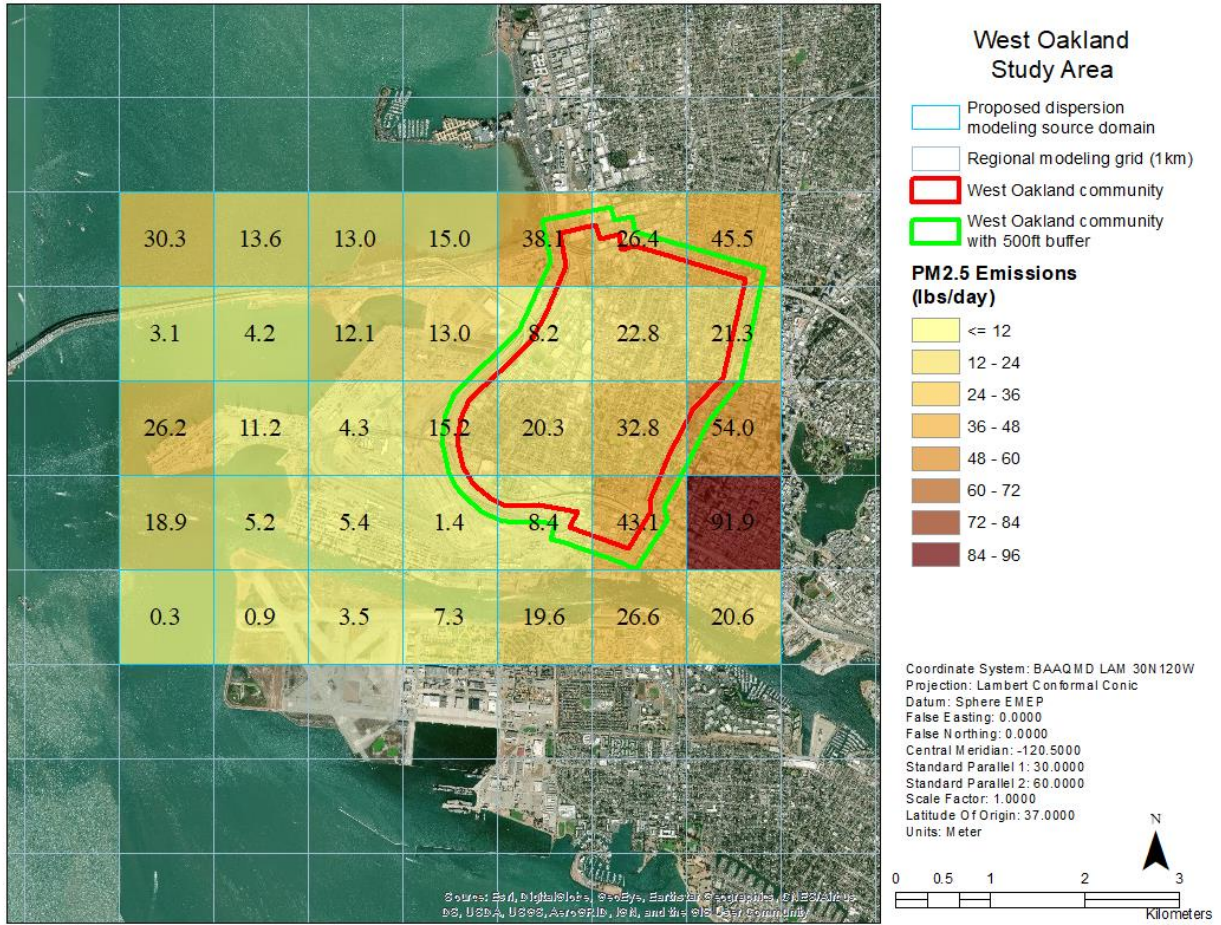


Figure 3.3: Spatial distribution of annual average PM_{2.5} emissions in West Oakland.

3.2 Meteorological Modeling

The Weather Research and Forecasting (WRF) Model version 3.8 was used to prepare meteorological inputs to CMAQ. Four nested modeling domains were used (Figure 3.4). The outer domain covered the entire western United States at 36-km horizontal grid resolution to capture synoptic (large-scale) flow features and the impact of these features on local meteorology. The second domain covered California and portions of Nevada at 12-km horizontal resolution to capture mesoscale (sub-regional) flow features and their impacts on local meteorology. The third domain covered Central California at 4-km resolution to capture localized air flow features. The 4-km domain included the Bay Area, San Joaquin Valley, and Sacramento Valley, as well as portions of the Pacific Ocean and the Sierra Nevada mountains. The fourth domain covered the Bay Area and surrounding regions at 1-km resolution. All four domains employed 50 vertical layers with thickness increasing with height from the surface to the top of the modeling domain (about 18 km).

Meteorological variables are estimated at the layer midpoints in WRF. The thickness of the lowest layer nearest the surface was about 25 m. Thus, meteorological variables near the surface were estimated for a height of about 12.5 m above ground level. The model configuration was tested using available physics options, including: (1) planetary boundary layer processes and time-based evolution of mixing heights; (2) choice of input database for WRF; (3) four-dimensional data assimilation (FDDA) strategy; (4) horizontal and vertical diffusion; (5) advection scheme; and (6) initial and boundary conditions. The final choice of options was the one proved to best characterize meteorology in the domain.

WRF was applied for 2016 to estimate parameters required by the air quality model, including hourly wind speed and direction, temperature, humidity, cloud cover, rain and solar radiation levels. Observations are assimilated into the model during the simulations to minimize the difference between simulations and real-world measurements. Two types of nudging methods were employed (analysis and observation). The NCEP North America Mesoscale (NAM) 12-km analyzed meteorological fields were used for analysis nudging as well as for initializing the model. The NCEP ADP Global Surface and Upper Air Observational Weather Data were used for observational nudging. A list of these stations for the 1-km domain is given in Appendix A.

The analysis nudging was applied to the 36-km and 12-km domains. Frequency of surface analysis nudging was every three hours, while the frequency of 3D analysis nudging was every six hours. The 3D analysis nudging of winds was performed over all model layers, but the 3D analysis nudging of temperature and humidity was limited to layers above the planetary boundary layer. The observation nudging of wind was applied to all four domains every three hours.

The WRF model was rigorously evaluated for accuracy. Observations used to evaluate WRF were taken from the EPA's Air Quality System, the BAAQMD meteorological network, and the National Climate Data Center. A list of these stations for the 1-km domain is given in Appendix A. Hourly and daily time series plots of observed and simulated wind, temperature

and humidity were generated at each observation station and compared to each other hour by hour and day by day. Simulated hourly areal plots of wind, temperature, humidity, planetary boundary layer height, pressure and other fields were generated and quantitatively compared against observations where observations were available.

WPS Domain Configuration

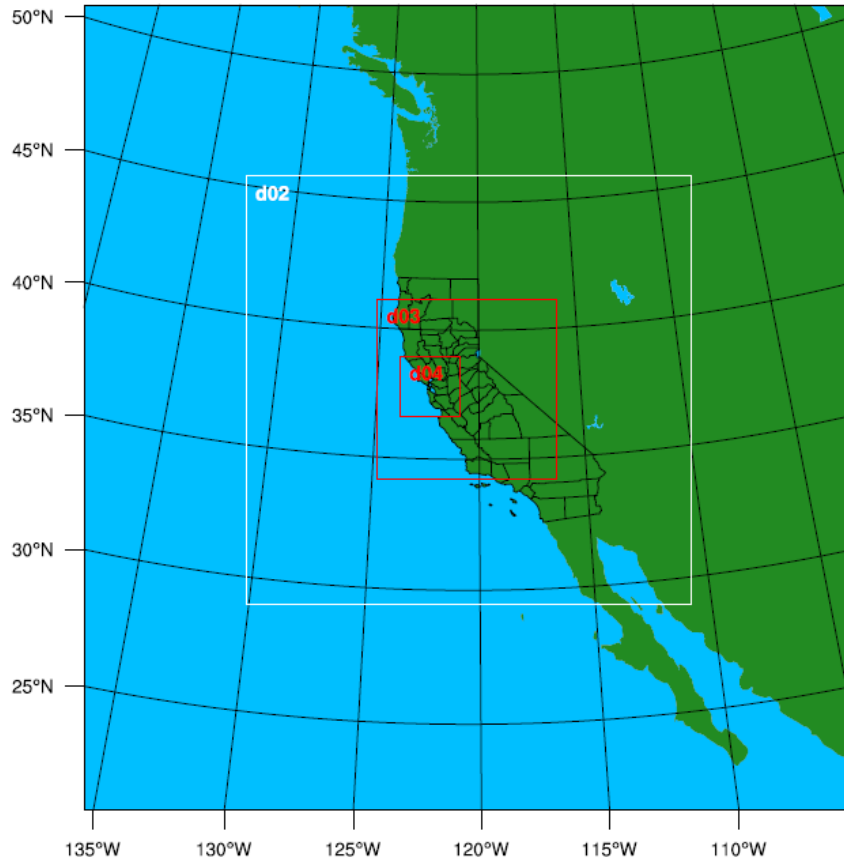


Figure 3.4: Nested WRF modeling domains.

These plots were also qualitatively evaluated for known meteorological features of the modeling domain, especially at 4-km and 1-km resolutions. These features include slope flows, channeled flows, sea breeze and low-level jet. The vertical profile of observed and simulated meteorological fields was compared at several upper air meteorological stations, including Oakland, Medford, Reno and Las Vegas, and at a temporary station established at Bodega Bay. RAMBOLL's METSTAT program (Emery et al., 2001) was used to statistically evaluate the performance of WRF. The statistical metrics used in this evaluation are defined in Appendix C.

The WRF model performed reasonably well in every evaluation category. The estimated bias, gross error, root mean square error (RMSE), and index of agreement (IOA) are within established criteria for acceptable model performance for every day of 2016. In other words,

performance obtained from the Bay Area applications of WRF is similar or slightly better than performance obtained from applications elsewhere, available from literature.

Performance statistics were generated for all days of 2016. Samples from ten winter (December 1-10) and ten summer (July 1-10) days are shown in Table 3.3, while Table 3.4 shows maximum and minimum skill scores of WRF for all of 2016.

Simulated and observed wind speed, wind direction, temperature and humidity, for both hourly and annual time periods, were compared at each station. Time series comparisons for West Oakland, Vallejo and San Jose are shown in Appendix C. These three stations were selected because West Oakland is the area of interest for this study. Vallejo is strategically located in the Delta to capture air flow between the Bay Area and the Central Valley. San Jose is an important sub-region of the Bay Area representing outflows. Good model performance at Vallejo and San Jose is critical to simulate representative meteorological features in West Oakland.

The WRF model was also compared against upper air measurements at Oakland, a site operated by the National Weather Service with twice daily upper air measurements and at Bodega Bay, a temporary site established by the California Baseline Ozone Transport Study with daily ozonesonde and meteorological measurements. Simulated winds, temperatures and humidity matched these upper air measurements very well. Details can be found in Appendix C.

Table 3.3: Sample (December 1-10 and July 1-10) statistical scores of WRF.

Parameter	Metric	Units	12/01	12/02	12/03	12/04	12/05	12/06	12/07	12/08	12/09	12/10
Wind Speed	Bias	(m/s)	-0.21	-0.43	-0.21	-0.68	-0.35	-0.38	-0.67	-0.32	-0.35	-0.77
Wind Speed	Gross Error	(m/s)	1.28	1.61	1.05	1.08	0.91	1.13	1.16	1.49	0.93	1.33
Wind Speed	RMSE	(m/s)	1.68	2.07	1.4	1.5	1.22	1.49	1.48	1.88	1.19	1.7
Wind Speed	IOA	-- ^a	0.78	0.75	0.64	0.67	0.66	0.73	0.71	0.7	0.66	0.79
Wind Direction	Bias	(deg)	2.21	-1.32	-6.78	3.74	4.73	13.09	3.22	5.08	-6.37	6.45
Wind Direction	Gross Error	(deg)	32.17	24.42	57.64	45.58	42.43	43.08	32.72	50.97	38.39	22.33
Temperature	Bias	(K)	1.26	1.25	2.6	0.85	0.35	1.76	2.08	0.75	-0.31	-0.68
Temperature	Gross Error	(K)	32.17	1.72	2.66	1.47	1.18	1.85	2.26	1.64	1.43	0.92
Temperature	RMSE	(K)	2.09	2.25	3.2	1.87	1.53	2.41	2.71	2.09	1.82	1.15
Temperature	IOA	-- ^a	0.93	0.91	0.87	0.94	0.94	0.88	0.82	0.89	0.88	0.87
Parameter	Metric	Units	7/01	7/02	7/03	7/04	7/05	7/06	7/07	7/08	7/09	7/10
Wind Speed	Bias	(m/s)	-0.96	-1.12	-0.96	-1.15	-1.04	-0.95	-1.08	-0.91	-1.27	-0.91
Wind Speed	Gross Error	(m/s)	1.35	1.48	1.37	1.53	1.44	1.43	1.51	1.41	1.7	1.44
Wind Speed	RMSE	(m/s)	1.81	1.91	1.77	2.02	1.99	1.86	2.01	1.8	2.26	1.88
Wind Speed	IOA	-- ^a	0.71	0.76	0.75	0.71	0.71	0.75	0.71	0.7	0.71	0.74

Wind Dir	Bias	(deg)	-0.16	0.36	-3.34	-1.97	-3.95	-1.52	0.97	3.73	3.51	4.82
Wind Dir	Gross Error	(deg)	28.1	27.05	24.63	27.85	24.76	23.07	20.44	21.91	21.83	28.44
Temperature	Bias	(K)	1.3	1.47	0.24	0.39	1.2	1.09	0.87	0.34	0.06	0.59
Temperature	Gross Error	(K)	1.89	1.9	1.21	1.14	1.58	1.36	1.12	1.14	0.87	1.17
Temperature	RMSE	(K)	2.43	2.34	1.56	1.48	1.99	1.69	1.39	1.43	1.09	1.54
Temperature	IOA	-- ^a	0.97	0.96	0.98	0.98	0.96	0.97	0.98	0.98	0.99	0.98

^aThe Index of Agreement (IOA) is a dimensionless quantity.

Table 3.4: Maximum and minimum statistical scores of WRF for 2016.

Parameter	Metric	Units	Max	Min
Wind Speed	Bias	(m/s)	1.02	-0.99
Wind Speed	Gross Error	(m/s)	2.03	0.57
Wind Speed	RMSE	(m/s)	2.5	0.76
Wind Speed	IOA	--	0.92	0.4
Wind Direction	Bias	(deg)	14.84	-12.56
Wind Direction	Gross Error	(deg)	81.37	13.5
Temperature	Bias	(K)	2.99	-1.62
Temperature	Gross Error	(K)	3.24	0.72
Temperature	RMSE	(K)	5.22	0.9
Temperature	IOA	--	0.98	0.47

3.3 Air Quality Modeling

Air quality modeling was conducted using the U.S. EPA’s Community Multiscale Air Quality (CMAQ) modeling system version 5.2. Two nested domains were used. The outer domain coincides with the third domain of the meteorological model and covers the Bay Area, San Joaquin Valley, and Sacramento Valley, as well as portions of the Pacific Ocean and the Sierra Nevada mountains at 4-km horizontal resolution. The inner domain covers the Bay Area and surrounding regions at 1-km horizontal resolution.

Both CMAQ modeling domains had 28 vertical layers. Below 1,500 m, the CMAQ layers match the WRF layers, while some upper-level meteorological model layers above 1,500 m were collapsed while preparing meteorological inputs for CMAQ to reduce computational time. This is a common practice in air quality modeling, as pollutant levels in layers aloft are relatively low and do not significantly impact concentrations at the surface. The thickness of CMAQ model layers was also increasing with height from the surface to the top of the modeling domain (about 18 km). The thickness of the first layer of CMAQ was kept the same as in WRF (about

25 m), meaning that pollutant concentrations are estimated at around 12.5 m above the surface (the midpoint of the first layer).

The outer domain provides initial conditions and hourly boundary conditions to the 1-km domain. As a result, the inner domain accounts for the contribution of emissions sources outside of the Bay Area to Bay Area PM levels. The outer domain was initialized and its boundary conditions were updated every six hours using outputs from a global air quality model (MOZART), available from the National Center for Atmospheric Research (NCAR).

CMAQ simulates both primary and secondary PM_{2.5}, with secondary PM_{2.5} formation being dependent upon photochemistry. The chemical mechanism used in this simulation was the Statewide Air Pollution Research Center version 2007 (SAPRC-07) mechanism. Secondary PM formulation was simulated using the Models-3 AE6 aerosol module.

Each month was simulated separately to distribute simulations over 12 computer nodes for computational efficiency. Each monthly simulation includes the last three days of the previous month as a spin-up period except for January, which includes the last five days of December 2015. Model outputs from the spin-up periods were not used in analyses.

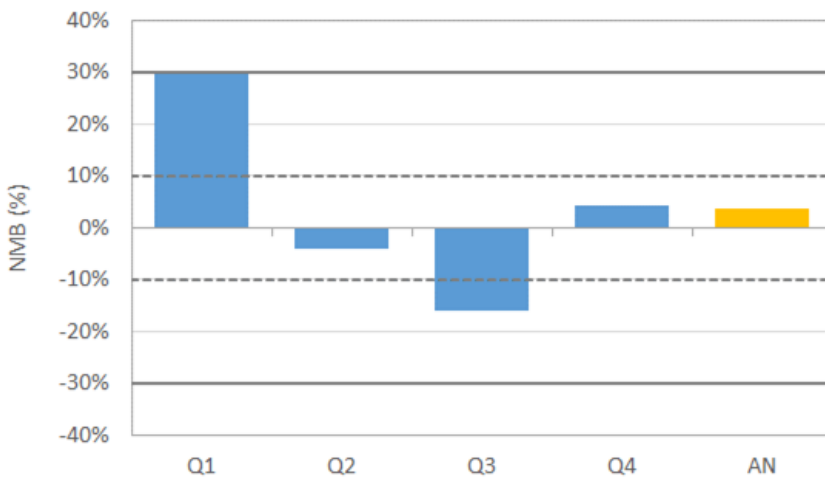
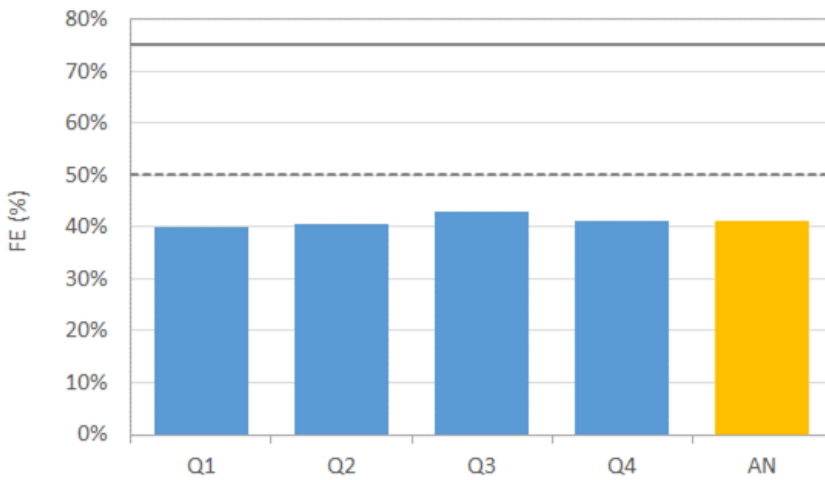
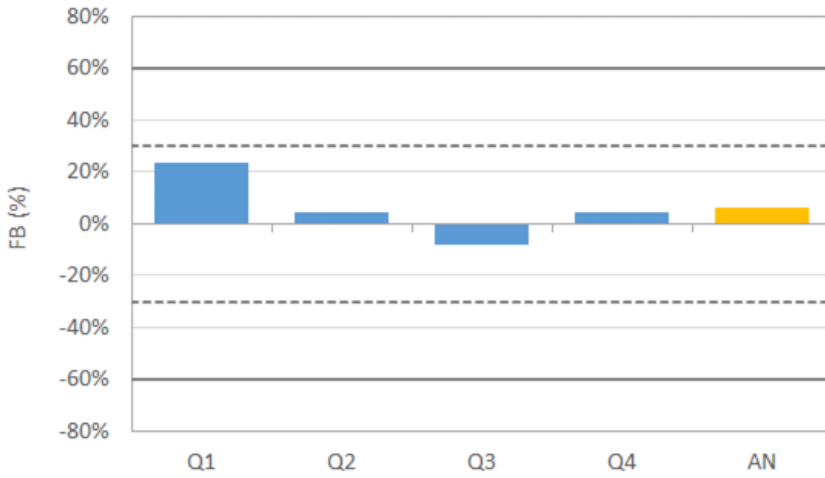
3.3.1 CMAQ Evaluation

The CMAQ model was rigorously evaluated for accuracy. Observations used to evaluate CMAQ were taken from the District's Data Management System and the EPA's Air Quality System. Hourly and daily time series plots of observed and simulated PM_{2.5} concentrations were generated at each observation station and compared to each other hour by hour and day by day. This evaluation also provided an opportunity to identify gaps in measurements and outliers. Hourly, daily, monthly, quarterly and annual average spatial plots of PM and precursor concentrations were generated for observed and simulated values, and simulated values were quantitatively compared against observations where observations were available.

These plots were also qualitatively evaluated for known air quality features that may be impacted by meteorology, emissions, chemistry and other environmental parameters. Examples include local and regional transport of pollutants, proximity of polluted areas to emission sources such as freeways, and the behavior of atmospheric chemistry.

Various statistical metrics were used to evaluate the performance of CMAQ. Standard statistical measures used for CMAQ evaluation are described in EPA's latest modeling guidance (EPA, 2018) and in Appendix D. These metrics were applied for daily average simulated PM_{2.5} concentrations over quarterly and annual periods. The CMAQ model performed reasonably well, meeting the performance goals proposed by Boylan and Russell (2006) and criteria by Emery et al. (2017), two well-known references for PM model evaluation. Figure 3.5 shows fractional bias, fractional error, normalized mean bias and normalized mean error for quarterly

and annual periods. The performance goals (dashed lines) and criteria (solid lines) are also shown in the figure as references.



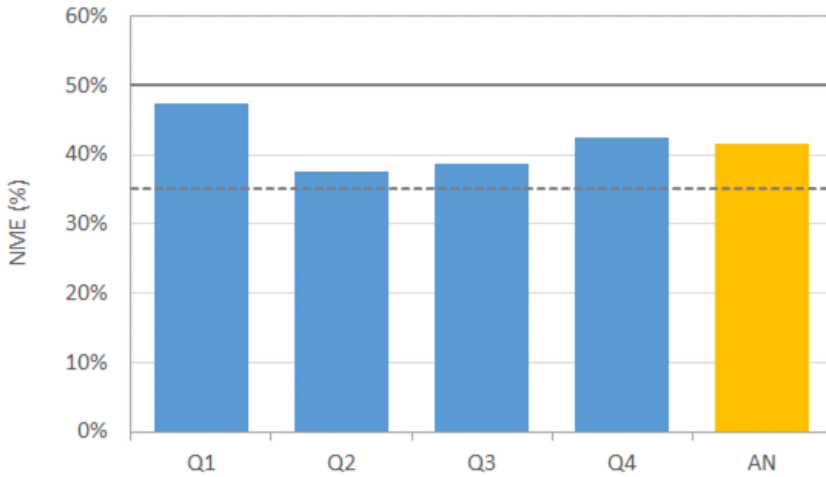


Figure 3.5: Quarterly and annual performance statistics for simulated PM_{2.5} over the 26 air monitoring sites within the 1-km modeling domain with performance goals (dashed lines) and criteria (solid lines) proposed by Boylan and Russell (2006) and Emery et al. (2017). FB stands for fractional bias, FE fractional error, NMB normalized mean bias and NME normalized mean error.

Additional comparisons between simulated and observed PM_{2.5} are discussed in Section 4 (Results) and in Appendix D. These comparisons largely focus on three selected Bay Area sites (West Oakland, Vallejo and San Jose) that are particularly relevant to West Oakland study.

4. Results

Comparison between the annual average simulated and observed PM_{2.5} concentrations (Figure 4.1) shows that the CMAQ model generally captured the observed PM_{2.5} pattern within the 1-km domain. High concentrations in both simulations and observations are evident in the northern San Joaquin Valley, along the I-580 and I-880 corridors from Richmond to the Oakland Airport, along the I-101 corridor near Redwood City, and in the San Jose metropolitan area. In the Sacramento area, the model shows overestimation biases and PM_{2.5} concentrations do not compare as well to observations as in the Bay Area. For Sacramento and other counties outside the Bay Area, we relied on the ARB's emission inventories, and further evaluation of these data may be warranted. The model also shows high concentrations along the I-880 corridor from Oakland Airport to San Jose and along the Delta from Antioch to Brentwood, although observations are unavailable in these areas.

Site by site comparisons between the model predictions and observations (Figure 4.2) show that at most Bay Area sites, the simulated annual average PM_{2.5} concentrations are within ± 1.0 $\mu\text{g}/\text{m}^3$ of observations. At a few sites (Concord, Oakland and Gilroy), the annual average PM_{2.5} concentrations were overestimated, and at one site (Napa), the annual average PM_{2.5} concentration was underestimated by as much as 2.1 $\mu\text{g}/\text{m}^3$.

Further analyses of model output showed that at sites with overestimated PM_{2.5}, both primary and secondary PM_{2.5} concentrations appear to be overestimated. This suggests that there may be multiple causes of overestimation. Primary PM_{2.5} concentrations can be overestimated due to overestimation of emissions, transport, and stability of the atmosphere. Secondary PM_{2.5} can be overestimated due to overestimation of precursor emissions, chemical conversion of the precursors to PM, transport of secondary PM_{2.5} or its precursors, and stability of the atmosphere.

Underestimation of PM_{2.5} at Napa is likely due to an underestimation of wood burning emissions or the transport of wildfire emissions to the North Bay. Wildfire emissions are not included in the modeling emissions inventory.

Figure 4.3 shows time-series plots of observed and simulated daily PM_{2.5} concentrations at three key Bay Area sites relevant to the West Oakland study: West Oakland, Vallejo and San Jose. It is evident from this figure that PM_{2.5} is generally overestimated during winter months and underestimated during summer months. However, on a monthly average basis, the CMAQ model is generally able to replicate the month-to-month variation in observed PM_{2.5} concentrations in West Oakland (Figure 4.4). The somewhat significant underestimation in September is likely due to lack of wildfire emissions in the CMAQ simulations.

During winter months, especially in February, the atmosphere is relatively sunny, calm and cool in the Bay Area, ideal conditions for the formation of secondary PM and for allowing

ammonium nitrate to remain in particle form. All of these suspected causes of overestimation are under further investigation and evaluation.

Wintertime overestimation and summertime underestimation of $PM_{2.5}$ by the WRF-CMAQ couple have also been reported elsewhere, and developers of the modeling system are aware of this problem (Appel et al., 2017; Simon et al., 2012). Efforts are underway by the model developers and District staff to minimize errors and to improve model performance for both winter and summer.

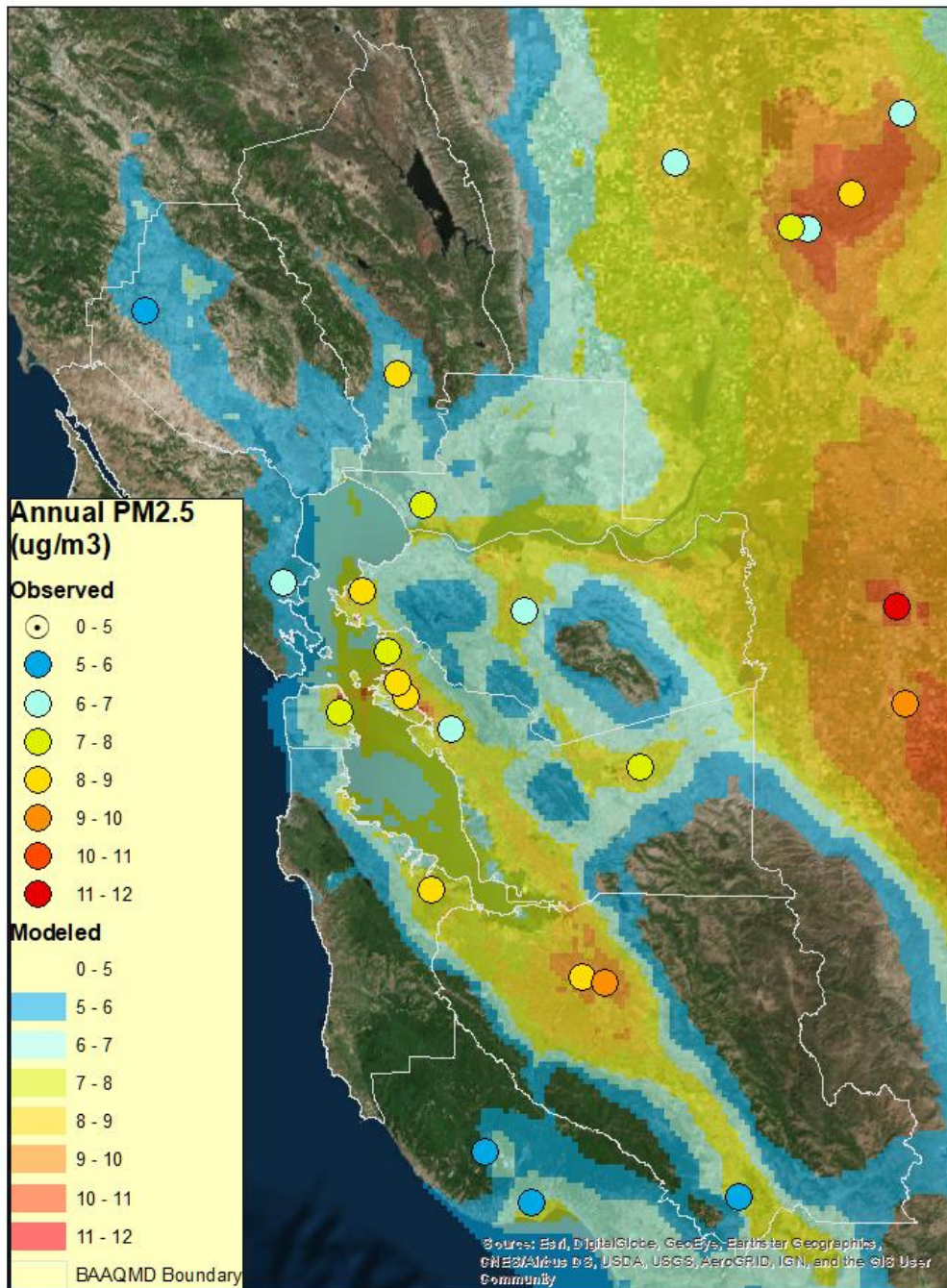


Figure 4.1: Spatial distribution of simulated and observed annual average PM_{2.5} concentrations within the 1-km modeling domain.

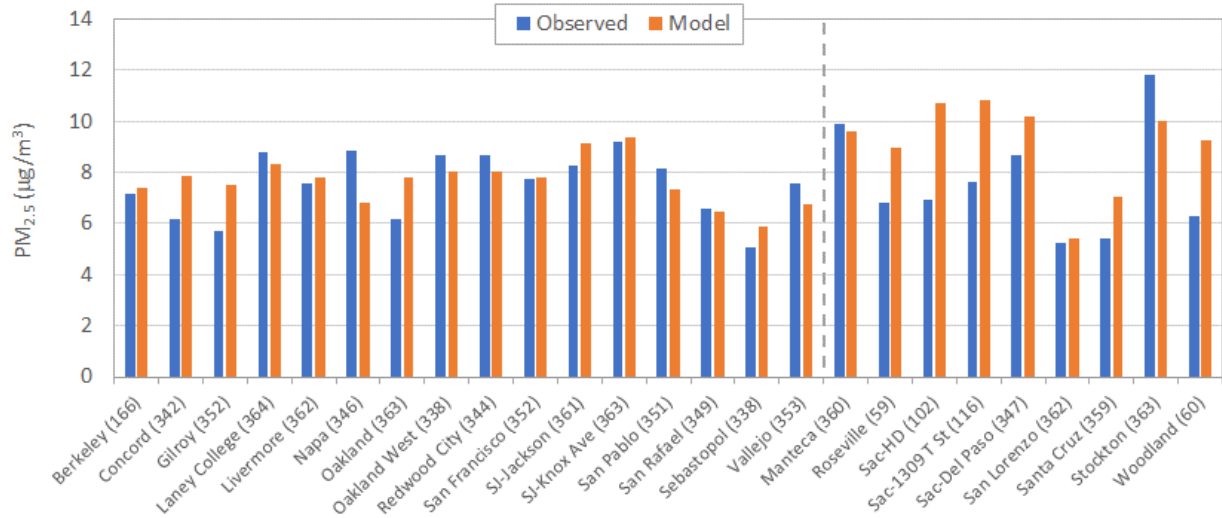
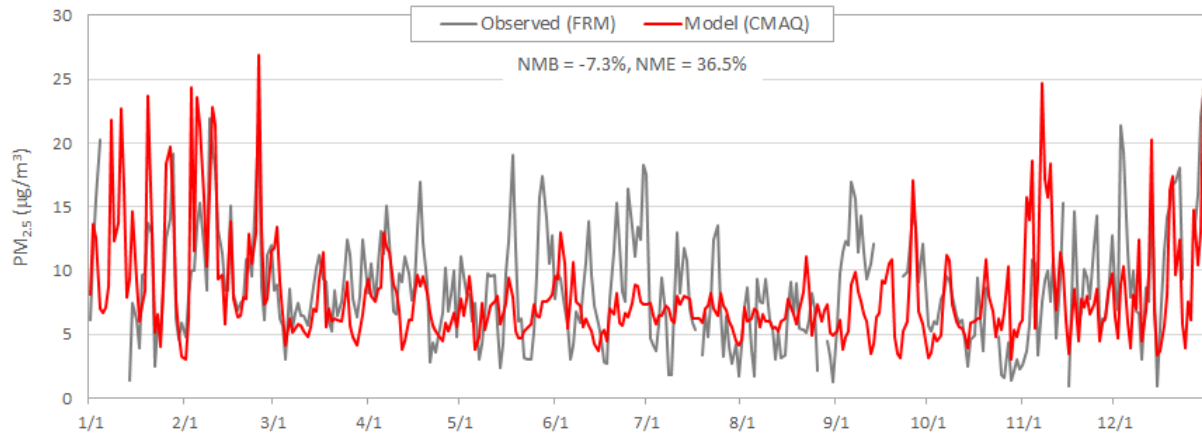
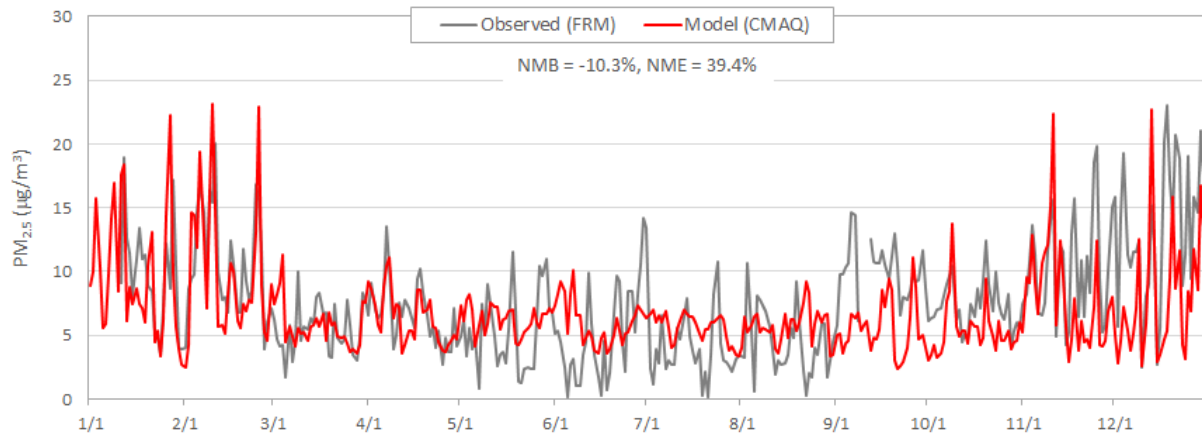


Figure 4.2: Annual mean observed vs. modeled PM_{2.5} concentrations at monitoring sites within the 1-km modeling domain. The annual means are calculated over the days with valid observations. The number of valid observations is shown in parentheses for each site. The Berkeley site is missing observations for January through June. Two Sacramento sites (Health Department - Stockton Blvd. and 1309 T Street) have observations every 3rd day. The Roseville and Woodland sites have observations every 6th day. The Sacramento - Bercut Drive site has data only for December, so its annual mean is not shown.

(a) Oakland West



(b) Vallejo



(c) San Jose – Knox Avenue

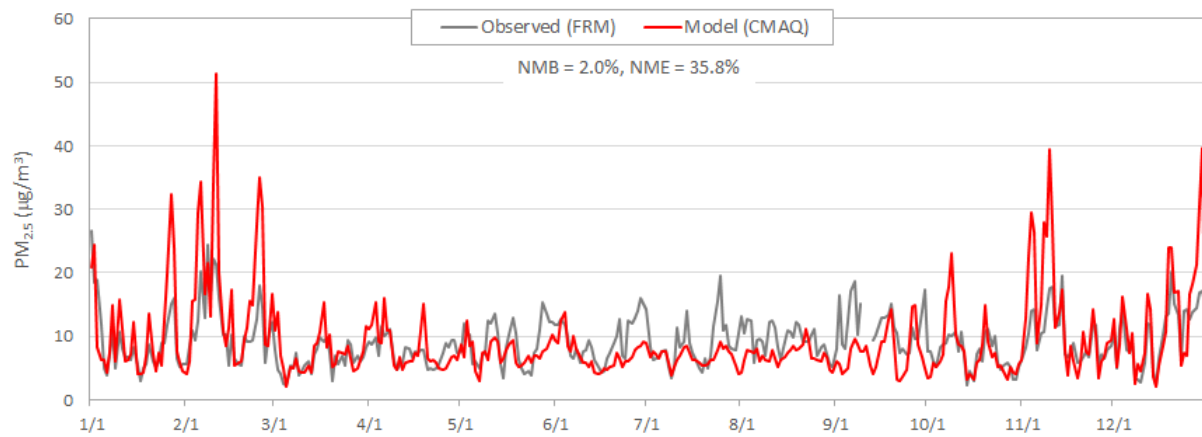


Figure 4.3: Time-series plots of observed vs. modeled daily PM_{2.5} concentrations at (a) Oakland West, (b) Vallejo, and (c) San Jose monitoring sites.

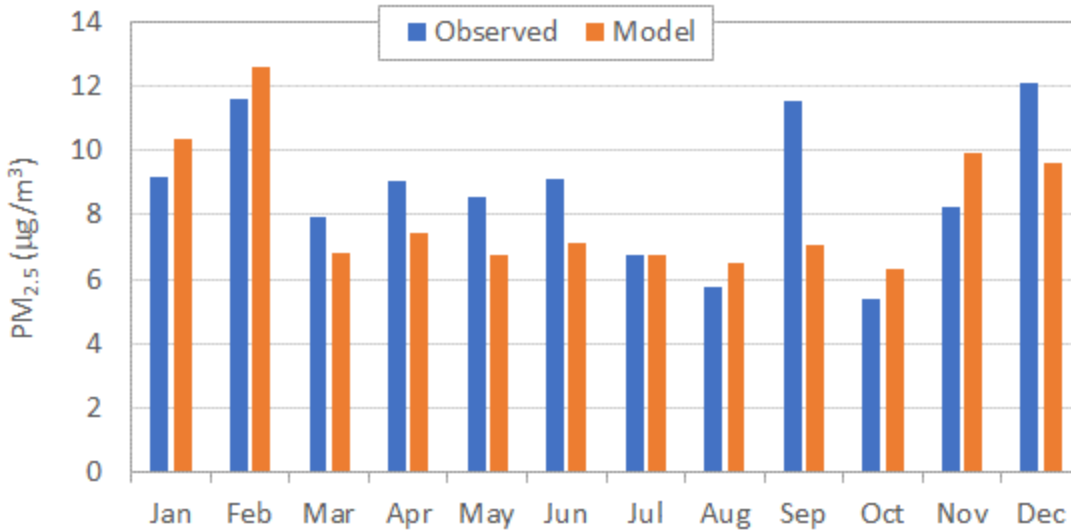


Figure 4.4: Monthly average simulated and observed PM_{2.5} concentrations in West Oakland.

4.1 Estimating Background PM_{2.5} in West Oakland

As mentioned in Section 1, we have simulated pollutant concentrations at a 1-km horizontal resolution over the entire Bay Area for 2016 (base case). Then we repeated the simulation with all anthropogenic emissions removed from the modeling inventory in the West Oakland source domain (control case), leaving all other model input parameters unchanged.

Figure 4.5 shows the annual average PM_{2.5} concentrations for the base case within the West Oakland receptor domain. The highest and lowest annual average PM_{2.5} concentrations are 9.3 µg/m³ and 7.1 µg/m³, respectively. A concentration gradient is evident within the domain. Cells with relatively higher concentrations extend along the eastern boundary and northwestern corner of the domain. A concentration gradient is also evident in the West Oakland community, an area within the red border in the figure. The eastern half of the community has slightly higher concentrations than the western half.

The spatial distribution of the annual average PM_{2.5} concentrations is similar to the spatial distribution of West Oakland's emissions (Figure 3.3). The Chinatown area in the southeastern corner of the West Oakland domain has the highest emissions and concentrations. The cell along the southern boundary with the area's lowest concentration (7.1 µg/m³) also has the lowest emissions (1.4 lbs/day).

Figure 4.6 shows the annual average PM_{2.5} concentrations for the control case, i.e., a simulation without West Oakland's anthropogenic emissions. Compared to Figure 4.5, the spatial gradient in the annual average concentrations decreased significantly in the absence of West Oakland emissions across the receptor domain. The location of the maximum annual average PM_{2.5} concentrations has shifted from Chinatown to near the Bay Bridge, suggesting the influence of transport from the northwest corner of the domain.

Figure 4.7 shows the difference between the base and control cases. Based on the figure, the Chinatown area would benefit the most ($2.5 \mu\text{g}/\text{m}^3$) from zeroing out all anthropogenic emissions in the West Oakland source domain. The West Oakland community (within the red border) would benefit by $\text{PM}_{2.5}$ reductions ranging from $0.8 \mu\text{g}/\text{m}^3$ to $1.7 \mu\text{g}/\text{m}^3$. The southwest corner of the receptor domain would be the least benefitted area, with a reduction of about $0.5 \mu\text{g}/\text{m}^3$.

Note that these $\text{PM}_{2.5}$ concentrations and reductions represent the average value across a 1×1 km grid cell. Higher concentrations and reductions are possible at the sub-grid cell level, and these finer-scale gradients will be investigated with local-scale AERMOD modeling.

Bias in the simulated annual average $\text{PM}_{2.5}$ concentrations for both base and control cases are expected to be similar. Since reductions are estimated from the difference between the two simulations, the impact of model bias on estimated reductions is expected to be insignificant.

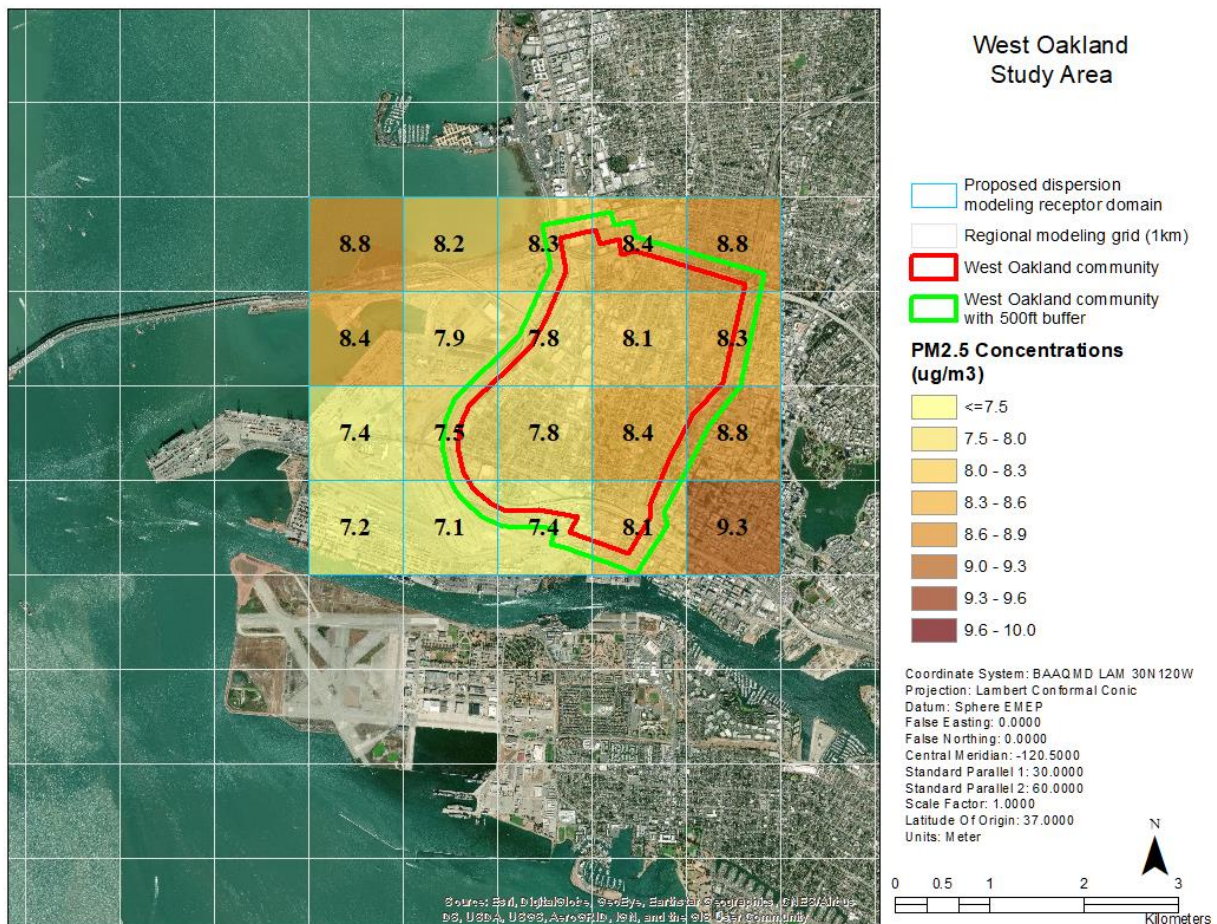


Figure 4.5: Spatial distribution of the simulated annual average $\text{PM}_{2.5}$ concentrations in the West Oakland receptor domain (base case).

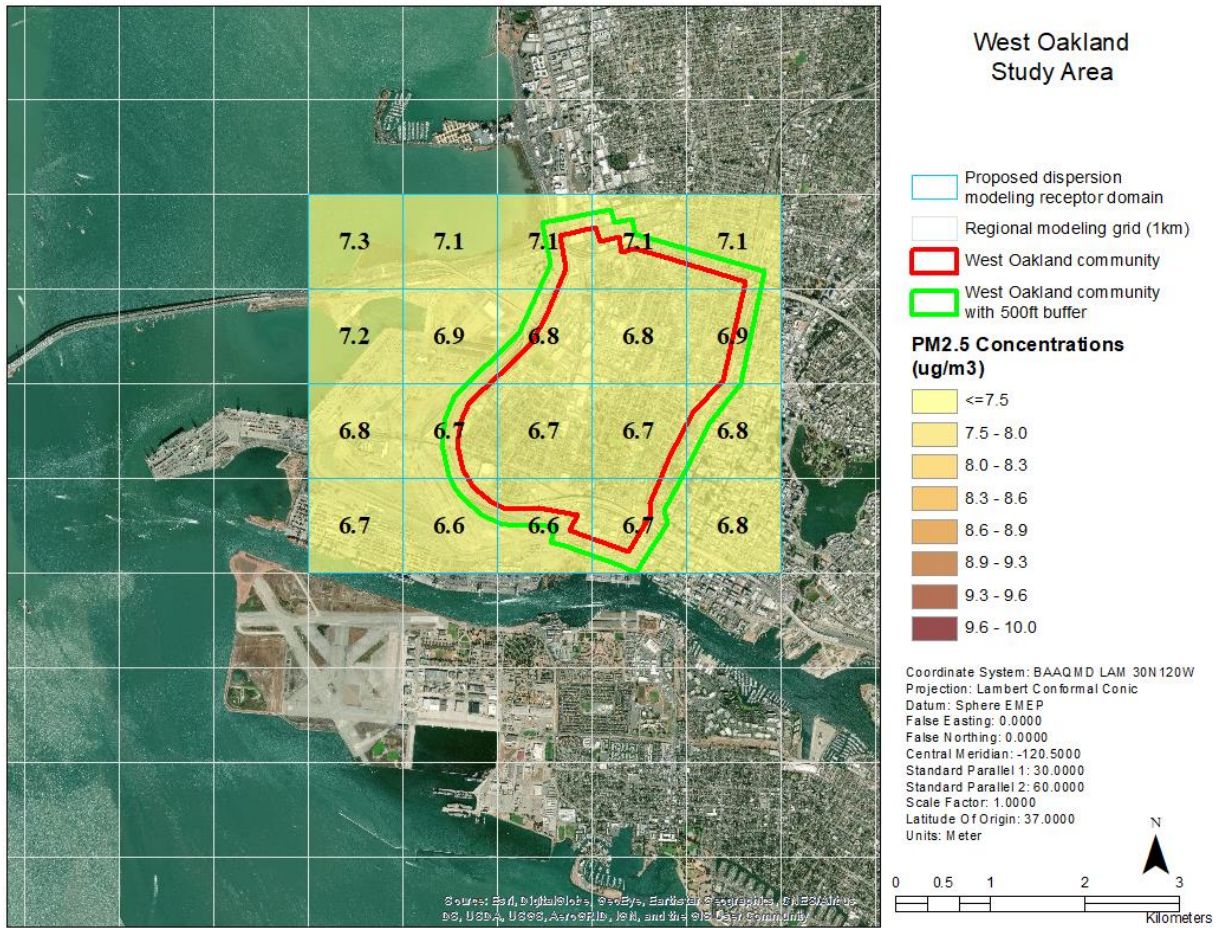


Figure 4.6: Spatial distribution of the simulated PM_{2.5} concentrations without West Oakland’s anthropogenic emissions (control case).

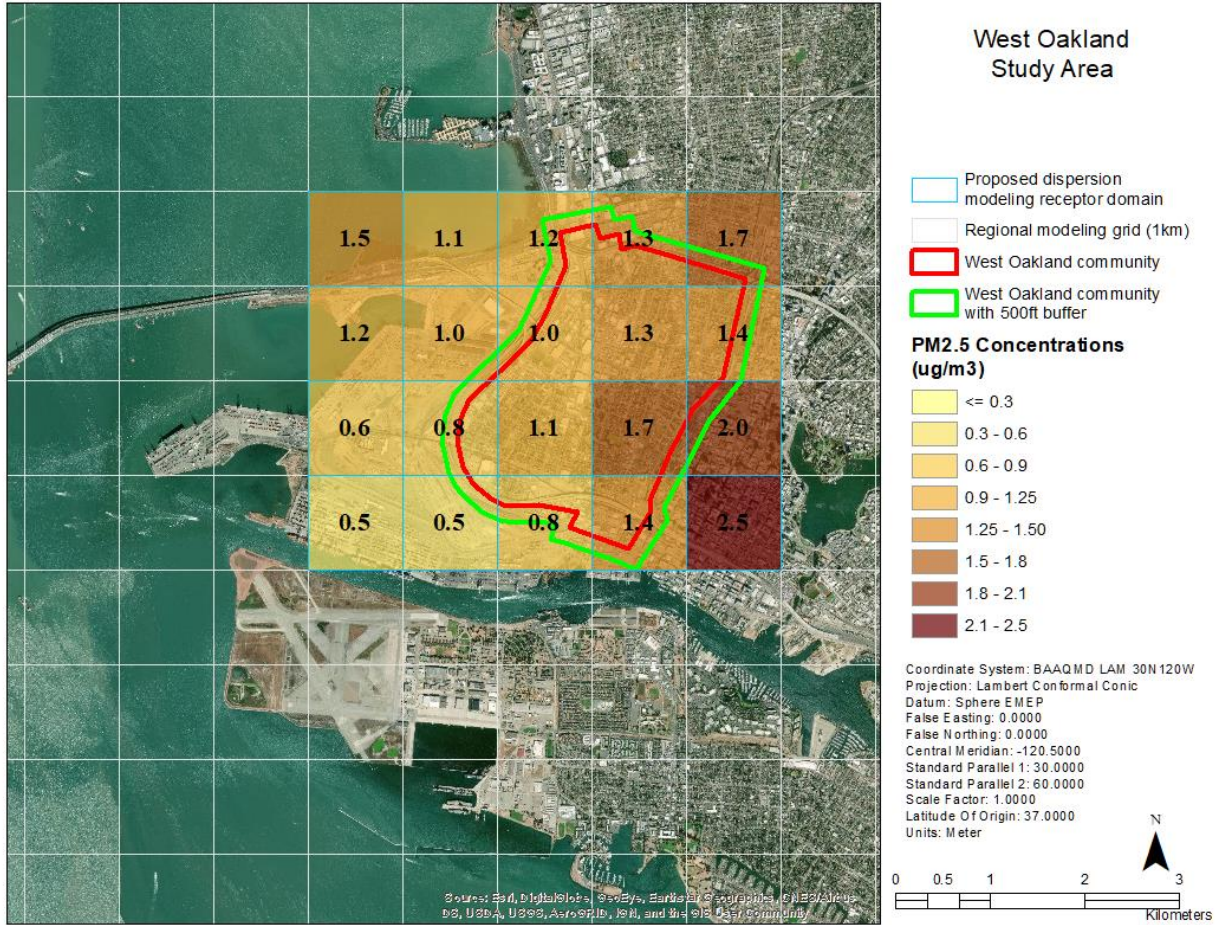


Figure 4.7: Difference between the simulated annual average base and control case PM_{2.5} concentrations.

Appendix A – Observational Data

A1. Description of Observations

Table A1 lists all aerometric stations within the 1-km modeling domain from which data were used in this study. It also shows data sources, data types, and purpose of the data. Under the monitoring location column, the first two subsections list PM_{2.5} stations within and outside of the Bay Area. The subsequent subsections list meteorological measurement stations within and outside of the Bay Area, followed by a list of upper air measurement stations. Meteorological measurement stations within the Bay Area are further separated based on whether or not they are operated by the District. Some stations measure both PM_{2.5} and meteorology. These stations are listed under both the PM_{2.5} and meteorology measurement sections and identified through checkmarks under columns titled “PM” and “Met.”

Hourly PM_{2.5} and meteorological data were obtained from the District’s Data Management System (DMS) in October 2018, and hourly PM_{2.5} and meteorological data were obtained from the U.S. EPA’s Air Quality System (AQS) at around the same time. Hourly meteorological data were also obtained from the NCAR/UCAR ADP data archive and twice daily upper air data were obtained from NOAA’s National Climatic Data Center.

The ADP and National Climatic Data Center data were used for the four-dimensional data assimilation (FDDA) in the WRF model. FDDA is a method to nudge the WRF model results towards observations. The WRF model includes a post-processing utility computer program that prepares the ADP and NCDC data for FDDA. The utility program also quality assures and quality checks both the ADP and National Climatic Data Center data. Meteorological data from the other sources listed in Table A1 were not used in FDDA because they do not include pressure, which is required for the nudging process. All the observed meteorological data listed in the column titled “Met” were used for WRF model validation using a software tool called METSTAT. The METSTAT program has a module for applying consistency checks to the data being used.

PM_{2.5} data obtained from DMS and AQS were compared against each other and no differences were found. PM_{2.5} data were used for both data analysis and CMAQ model validation. For consistency in data format, only data downloaded from AQS were used for data analysis and model validation.

As explained in the main text of this document, time series and spatial plots of simulated and observed hourly PM_{2.5} concentrations were generated and compared against each other. This process allowed identification of gaps and outliers in the PM_{2.5} data. Statistical formulas were developed in an Excel spreadsheet to evaluate the observations, such as assessing gaps in measurements, calculating daily, monthly, seasonal and annual averages, and assessing high and low values. Statistical formulas were also developed to assess bias, normalized bias and root mean square error in simulations by comparing simulated values to observations.

Table A1: Description of observations used in this study.

Monitoring Location	Source	PM	Met (ws, wd, t, rh)*	FDDA	Model Validation	
					WRF	CMAQ
<i>San Francisco Bay Area PM Stations</i>						
Berkeley Aquatic Park	DMS	x				x
Concord	DMS	x	x			x
Gilroy	DMS	x				x
Laney College	DMS	x				x
Livermore	DMS	x	x			x
Napa	DMS	x	x			x
Oakland	DMS	x				x
Oakland West	DMS	x				x
Redwood City	DMS	x				x
San Francisco	DMS	x				x
San Jose - Jackson	DMS	x				x
San Jose - Knox Avenue	DMS	x				x
San Pablo	DMS	x				x
San Rafael	DMS	x				x
Sebastopol	DMS	x				x
Vallejo	DMS	x	x			x
<i>PM Stations Outside the San Francisco Bay Area</i>						
Manteca	AQS	x				x
Roseville - N Sunrise Ave	AQS	x	x			x
Sacramento Health Department - Stockton Blvd.	AQS	x				x
Sacramento - 1309 T Street	AQS	x	x			x
Sacramento - Bercut Drive	AQS	x				x
Sacramento - Del Paso Manor	AQS	x	x			x
San Lorenzo Valley Middle School	AQS	x				x
Santa Cruz	AQS	x				x
Stockton - Hazelton	AQS	x	x			x
Woodland - Gibson Road	AQS	x				x
<i>BAAQMD Met Stations</i>						
Bethel Island	DMS		x		x	
Chabot	DMS		x		x	
Concord	DMS	x	x		x	
Fairfield	DMS		x		x	
Ft. Funston	DMS		x		x	
Livermore	DMS	x	x		x	
Napa	DMS	x	x		x	
Oakland STP	DMS		x		x	
Patterson Pass	DMS		x		x	
Pleasanton	DMS		x		x	
Pt. San Pablo	DMS		x		x	

Monitoring Location	Source	PM	Met (ws, wd, t, rh)*	FDDA	Model Validation	
					WRF	CMAQ
Rio Vista	DMS		x		x	
San Carlos	DMS		x		x	
San Martin	DMS		x		x	
San Ramon	DMS		x		x	
Sonoma Baylands	DMS		x		x	
Vallejo	DMS	x	x		x	
Valley Ford	DMS		x		x	
<i>Non-BAAQMD Met Stations in the Bay Area</i>						
Berkeley Lab	DMS		x		x	
Concord KCCR	ADP		x	x	x	
Hayward KHWD	ADP		x	x	x	
Livermore KLVK	ADP		x	x	x	
Moffett NASA/Mountain View KNUQ	ADP		x	x	x	
Napa KAPC	ADP		x	x	x	
Novato KDVO	ADP		x	x	x	
Oakland KOAK	ADP		x	x	x	
Palo Alto KPAO	ADP		x	x	x	
Petaluma KO69	ADP		x	x	x	
San Carlos KSQL	ADP		x	x	x	
San Francisco KSFO	ADP		x	x	x	
San Francisco STP	DMS		x		x	
San Jose KSJC	ADP		x	x	x	
San Jose/Reid KRHV	ADP		x	x	x	
San Martin KE16	ADP		x	x	x	
Santa Rosa KSTS	ADP		x	x	x	
Travis AFB KSUU	ADP		x	x	x	
<i>Met Stations Outside the Bay Area</i>						
Davis - UCD Campus	AQS		x		x	
Davis KEDU	ADP		x	x	x	
Elk Grove - Bruceville Road	AQS		x		x	
Half Moon Bay KHAF	ADP		x	x	x	
Hollister KCVH	ADP		x	x	x	
Lincoln KLHM	ADP		x	x	x	
Mather Field KMHR	ADP		x	x	x	
McClellan AFB KMCC	ADP		x	x	x	
Modesto KMOD	ADP		x	x	x	
Roseville - N Sunrise Ave	AQS	x	x		x	
Sacramento - 1309 T Street	AQS	x	x		x	
Sacramento - Del Paso Manor	AQS	x	x		x	
Sacramento KSAC	ADP		x	x	x	
Salinas KSNS	ADP		x	x	x	
Sanford MUNI KSMF	ADP		x	x	x	

Monitoring Location	Source	PM	Met (ws, wd, t, rh)*	FDDA	Model Validation	
					WRF	CMAQ
Stockton KSCK	ADP		x	x	x	
Stockton - Hazelton	AQS	x	x		x	
Tracy - Airport	AQS		x		x	
Vacaville KVCB	ADP		x	x	x	
Watsonville KWVI	ADP		x	x	x	
<i>Upper Air Stations</i>						
Oakland Sounding	NCDC		x	x	x	

*ws=wind speed; wd=wind direction; t=temperature; rh=relative humidity.

A2. Spatial Distribution of Observation Stations

Figure A1 shows spatial distribution of meteorological observation stations in the 1-km modeling domain. They are grouped based on whether they are operated by BAAQMD or other agencies (non-BAAQMD) and whether they are inside or outside of the District boundaries. BAAQMD sites collocated with PM_{2.5} measurements are also marked.

The spatial distribution of PM_{2.5} monitoring stations in the 1-km modeling domain is shown in Figure A2. These stations are grouped based on whether they are inside or outside of the District boundaries. All stations within the District are operated by the District.

Note that both the meteorological and air quality models have nested domains. Meteorological and air quality measurements outside of the 1-km domain were obtained from various databases and used for FDDA and model evaluation along with data for the 1-km domain. These data are stored on modeling computers and are available on request.

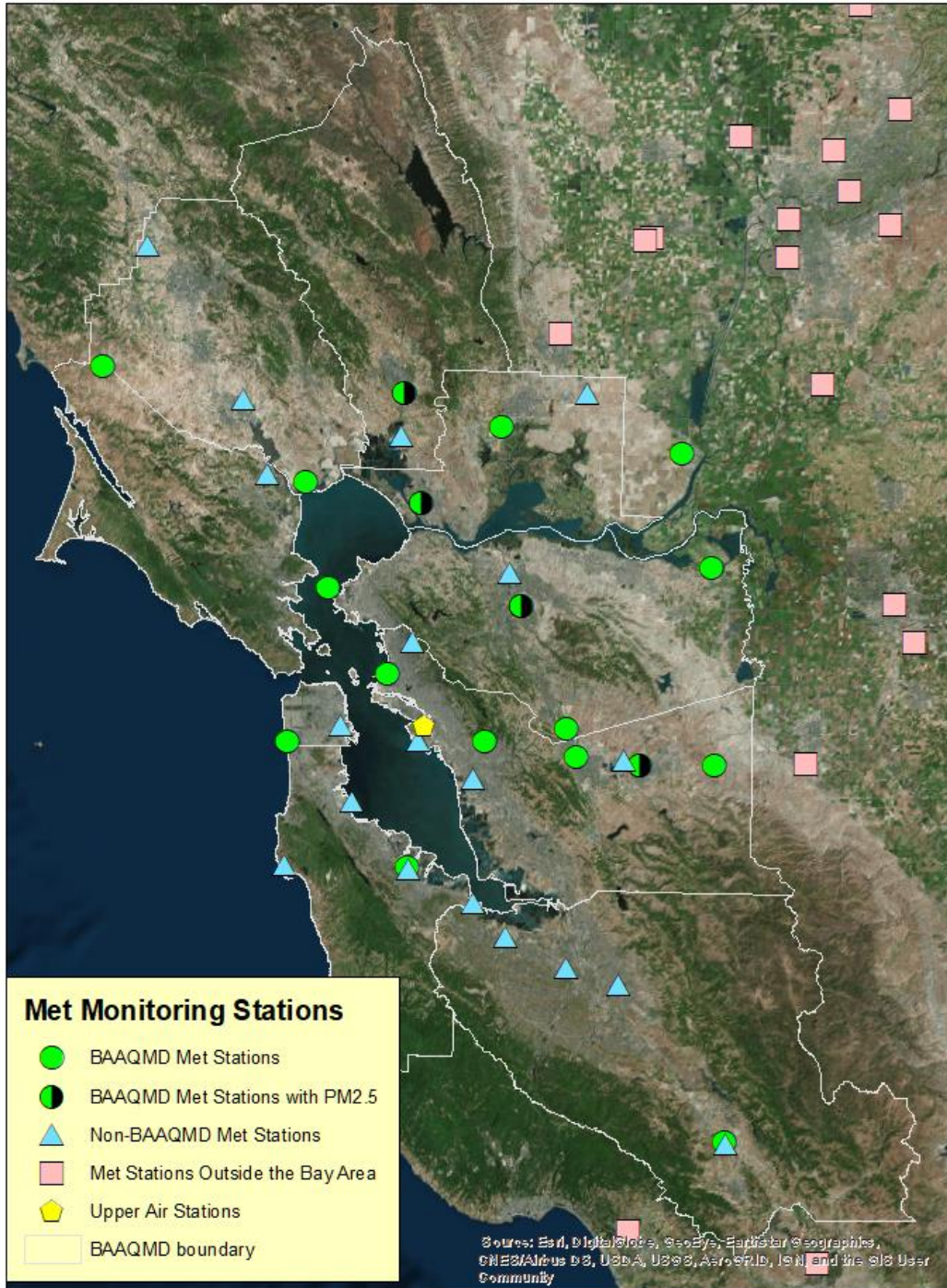


Figure A1: Spatial distribution of meteorological monitoring sites in the 1-km modeling domain.

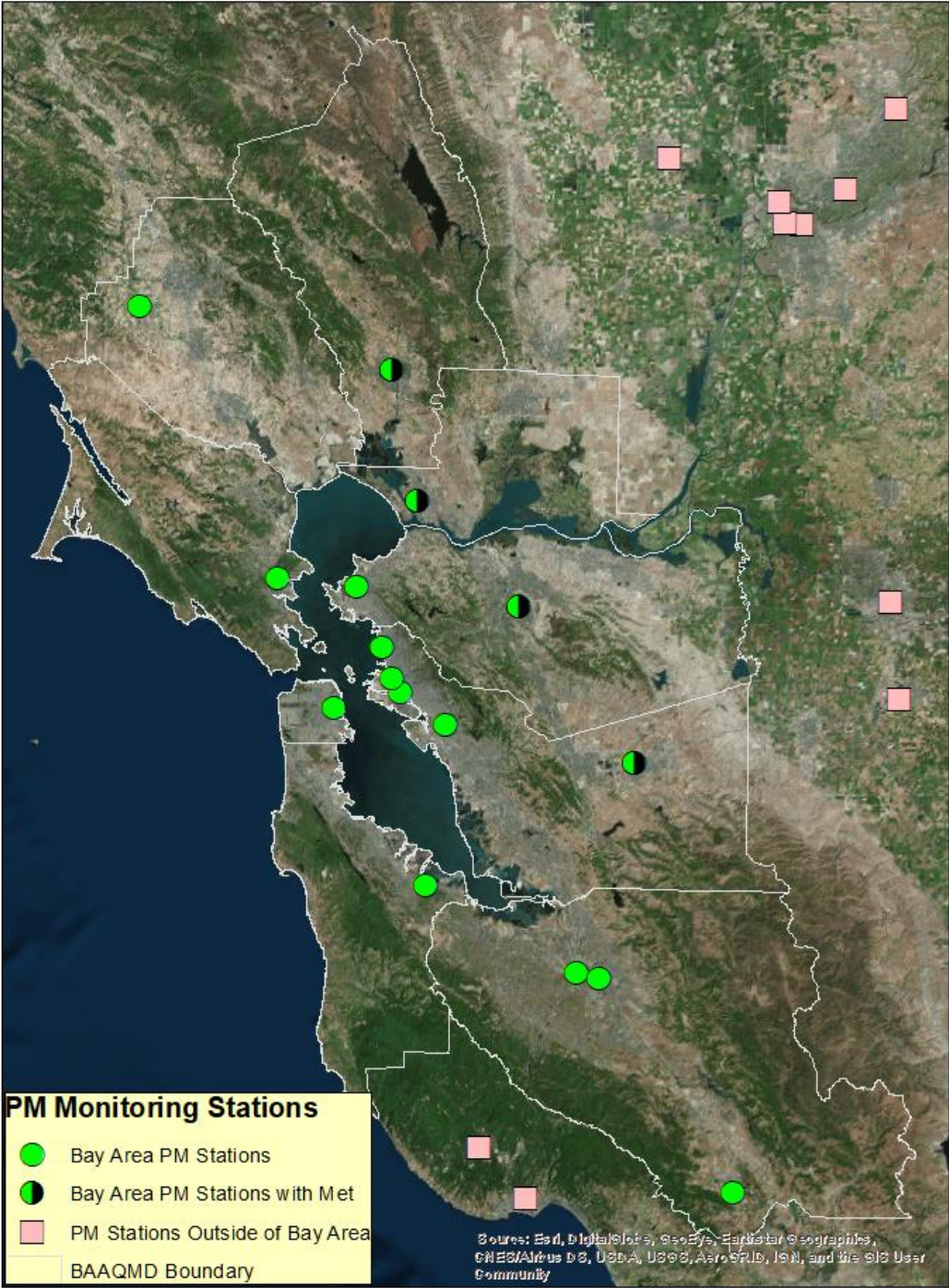


Figure A2: Spatial distribution of PM_{2.5} monitoring stations in the 1-km modeling domain.

Appendix B – Emissions Inventory

This appendix provides additional details on the development of emissions estimates for residential wood combustion, an important PM_{2.5} source during winter pollution episodes. This appendix also contains additional summary tables and emissions density plots that characterize the emissions inventory used for the 2016 CMAQ modeling.

B1. Residential Wood Combustion

ARB emissions estimates for residential wood combustion are based on county-level populations of fireplaces and woodstoves, wood consumption rates by device type, and emission factors that represent the quantity of emissions per ton of fuel burned. Where possible, ARB estimates device populations and wood consumption rates using local survey data, such as data collected as part of the District's Spare the Air Tonight Study (BAAQMD, 2007). ARB residential wood combustion emissions estimates for the District were compared to internal estimates derived from survey data, as well as estimates from neighboring air districts.

Figure B1 shows annual average PM_{2.5} emissions from residential wood combustion for the two BAAQMD inventories, as well as inventories for the Sacramento Metropolitan Air Quality Management District (SMAQMD) and the San Joaquin Valley Unified Air Pollution Control District (SJVUAPCD). The internal BAAQMD inventory is somewhat higher than the ARB inventory for BAAQMD, and both BAAQMD inventories are significantly higher than emissions estimates for SMAQMD and SJVUAPCD. After additional investigations and discussions with ARB, it was determined that:

- ARB's PM_{2.5} emissions estimates for winter compared well with the District's internal estimates; however, the District's estimates for summer (which were extrapolated from winter survey results based on temperature data) are significantly higher than ARB's estimates. These summer estimates do not appear to be realistic and result in the higher annual average PM_{2.5} emissions in the District's internal inventory.
- Higher residential wood combustion emissions estimates for BAAQMD relative to SMAQMD and SJVUAPCD likely result from a failure to account for the impact of the District's Spare the Air Program.

Based on these findings, it was decided that ARB's residential wood combustion estimates for the District would be reduced by 50% as an initial estimate of the impact of the District's Spare the Air program. Figure B2 shows the final monthly average PM_{2.5} emissions from residential wood combustion that were included in the CMAQ modeling inventories. Monthly average emissions range from 0.20 tpd in August to 8.39 tpd in January, with an annual average of 3.93 tpd.

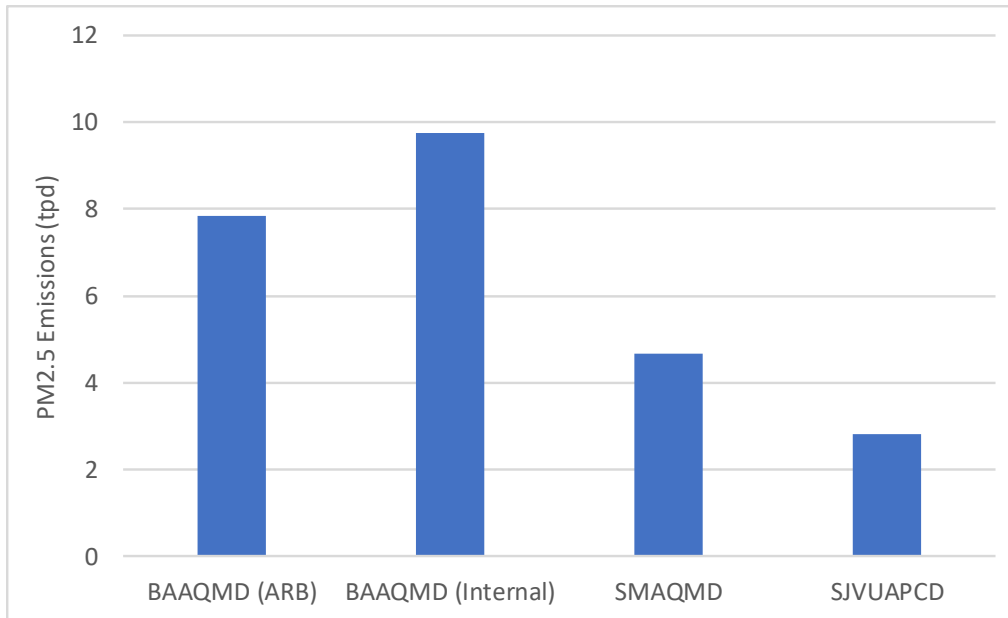


Figure B1: Comparison of 2016 annual average PM_{2.5} emissions inventories for residential wood combustion.



Figure B2: 2016 monthly average PM_{2.5} emissions for BAAQMD from residential wood combustion.

B2. Emissions Inventory Summaries

This section provides additional summary information on the emissions inventory used for the 2016 CMAQ modeling. Tables B1 through B4 show emissions of PM_{2.5} precursors (TOG, NO_x, SO₂, and NH₃) by geographic area and source sector. Key sources of TOG emissions include landfills, natural gas transmission losses, petroleum refining, and solvent usage. Key sources of NO_x emissions include onroad and nonroad mobile sources, especially diesel-powered vehicles.

Key sources of SO₂ emissions include petroleum refining and ocean-going vessels. Key sources of NH₃ emissions include farming operations such as livestock waste and fertilizer application.

Table B1: Summary of 2016 TOG emissions (tons/day) by geographic area and source sector.

Geographic Area	Area	Nonroad	Onroad	Point	Total
Alameda	42.6	8.0	12.4	64.1	127.1
Contra Costa	51.0	6.3	7.7	43.9	109.0
Marin	16.2	2.9	2.5	15.2	36.8
Napa	6.8	1.9	1.4	3.6	13.6
San Francisco	18.1	6.2	2.9	3.0	30.2
San Mateo	18.9	7.1	4.4	25.1	55.5
Santa Clara	57.6	8.1	12.2	50.8	128.7
Solano	14.3	2.1	2.6	8.7	27.7
Sonoma	25.4	3.0	3.5	9.1	41.1
<i>BAAQMD Subtotal</i>	<i>251.0</i>	<i>45.6</i>	<i>49.6</i>	<i>223.4</i>	<i>569.6</i>
Non-BAAQMD Counties	502.5	22.7	29.0	80.9	635.1
Domain Total	753.5	68.3	78.6	304.3	1,204.7

Table B2: Summary of 2016 NO_x emissions (tons/day) by geographic area and source sector.

Geographic Area	Area	Nonroad	Onroad	Point	Total
Alameda	3.4	12.0	27.2	3.2	45.8
Contra Costa	4.3	11.8	13.8	15.5	45.4
Marin	0.9	3.8	3.6	0.3	8.5
Napa	0.3	2.2	3.0	0.2	5.7
San Francisco	2.1	34.4	4.5	1.4	42.4
San Mateo	2.1	18.9	6.7	0.7	28.5
Santa Clara	4.2	10.0	22.2	8.5	45.0
Solano	1.0	3.9	5.4	3.8	14.1
Sonoma	0.9	7.9	6.7	0.4	15.9
<i>BAAQMD Subtotal</i>	<i>19.3</i>	<i>104.8</i>	<i>93.0</i>	<i>34.0</i>	<i>251.2</i>
Non-BAAQMD Counties	19.0	37.3	60.5	4.2	121.1
Domain Total	38.4	142.1	153.5	38.3	372.3

Table B3: Summary of 2016 SO₂ emissions (tons/day) by geographic area and source sector.

Geographic Area	Area	Nonroad	Onroad	Point	Total
Alameda	0.1	0.4	0.2	1.4	2.0
Contra Costa	0.1	0.9	0.1	16.6	17.7
Marin	0.0	0.0	0.0	0.1	0.2
Napa	0.0	0.0	0.0	0.0	0.0
San Francisco	0.1	0.4	0.0	0.1	0.6
San Mateo	0.1	0.9	0.1	0.1	1.1
Santa Clara	0.1	0.1	0.2	2.9	3.3
Solano	0.0	0.2	0.0	0.4	0.6

Sonoma	0.0	0.1	0.0	0.0	0.2
<i>BAAQMD Subtotal</i>	<i>0.5</i>	<i>3.1</i>	<i>0.7</i>	<i>21.6</i>	<i>25.9</i>
Non-BAAQMD Counties	1.6	0.3	0.4	1.9	4.2
Domain Total	2.1	3.4	1.1	23.4	30.1

Table B4: Summary of 2016 NH₃ emissions (tons/day) by geographic area and source sector.

Geographic Area	Area	Nonroad	Onroad	Point	Total
Alameda	3.0	0.0	1.5	0.4	4.9
Contra Costa	3.1	0.0	0.9	2.1	6.1
Marin	2.5	0.0	0.3	0.3	3.0
Napa	0.5	0.0	0.2	0.1	0.8
San Francisco	1.4	0.0	0.3	0.0	1.7
San Mateo	1.3	0.0	0.5	0.2	2.1
Santa Clara	3.6	0.0	1.6	1.5	6.7
Solano	1.9	0.0	0.3	0.1	2.3
Sonoma	3.3	0.0	0.4	0.3	4.0
<i>BAAQMD Subtotal</i>	<i>20.7</i>	<i>0.1</i>	<i>6.0</i>	<i>5.0</i>	<i>31.7</i>
Non-BAAQMD Counties	46.9	0.0	3.3	7.0	57.3
Domain Total	67.6	0.1	9.3	12.0	89.0

B3. Emissions Density Plots

This section provides emissions density plots that show the spatial distribution of key PM_{2.5} precursors (an emissions density plot for primary PM_{2.5} is provided in the main body of this report in Figure 3.1). The emissions density plot for NO_x (Figure B3) shows elevated emissions along major freeways and shipping lanes and in urban cores. Note that high emissions along shipping lanes in San Pablo Bay to the south of Marin County may be overestimated due to the spatial surrogate used for commercial marine vessel emissions, which does not include offshore shipping lanes for Sonoma County.

The emissions density plot for SO₂ (Figure B4) shows the presence of point sources in the 1-km domain that emit this pollutant, as well as emissions from commercial marine vessels along shipping lanes. The emissions density plot for NH₃ (Figure B5) shows elevated emissions in San Joaquin County in the eastern part of the modeling domain, an area with significant agricultural activity.

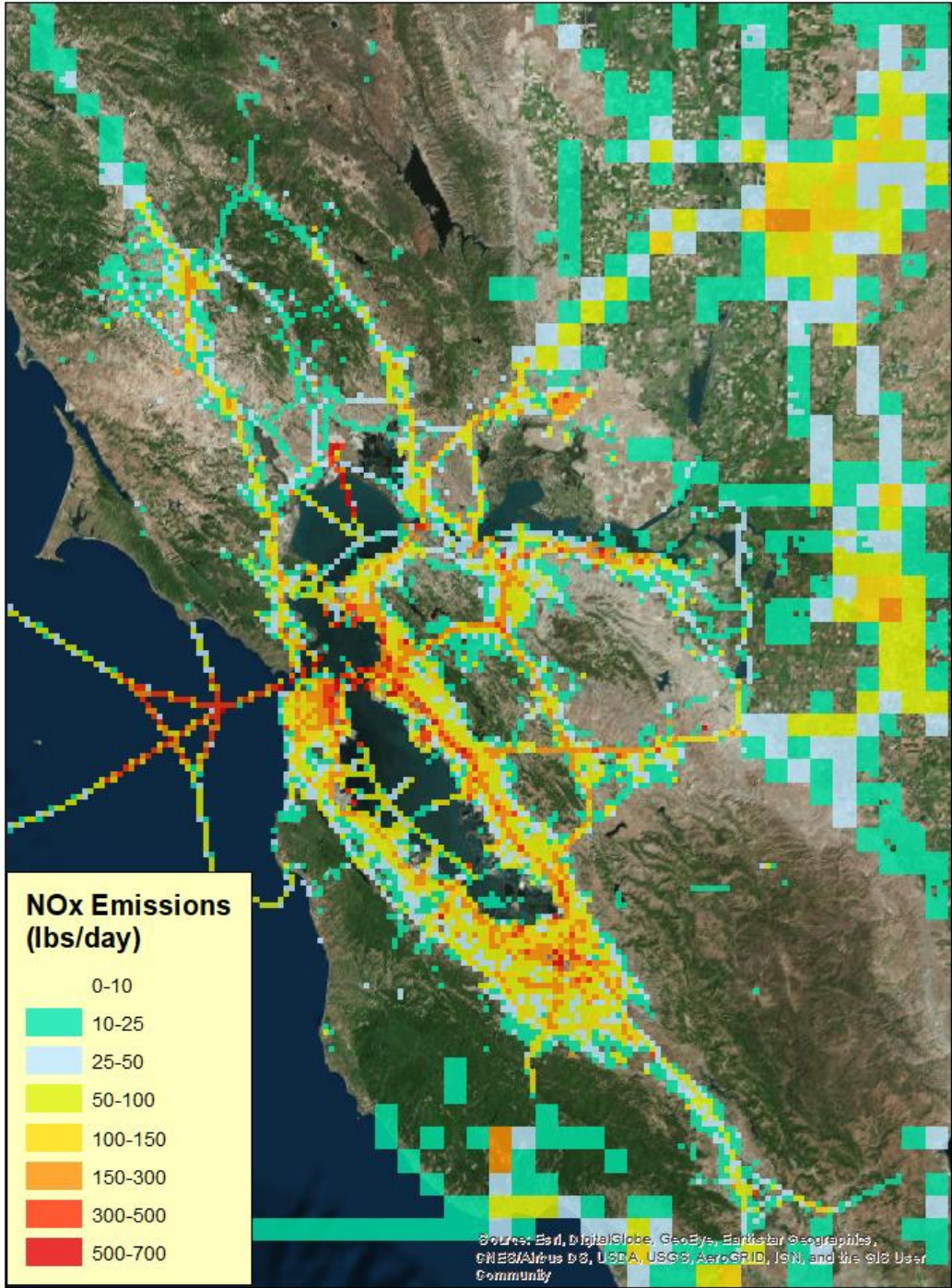


Figure B3: Spatial distribution of annual average NO_x emissions for the 1-km modeling domain.

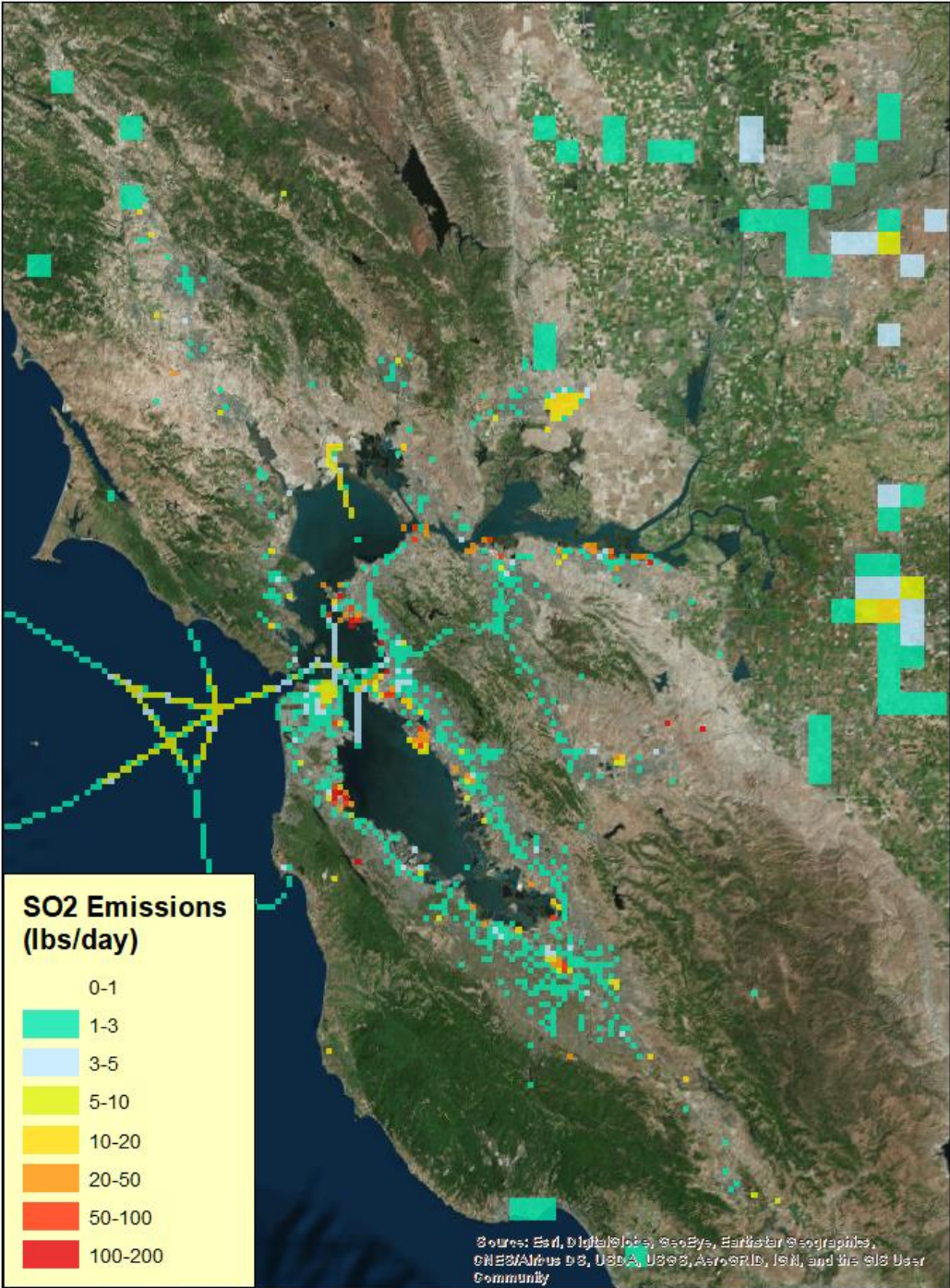


Figure B4: Spatial distribution of annual average SO₂ emissions for the 1-km modeling domain.

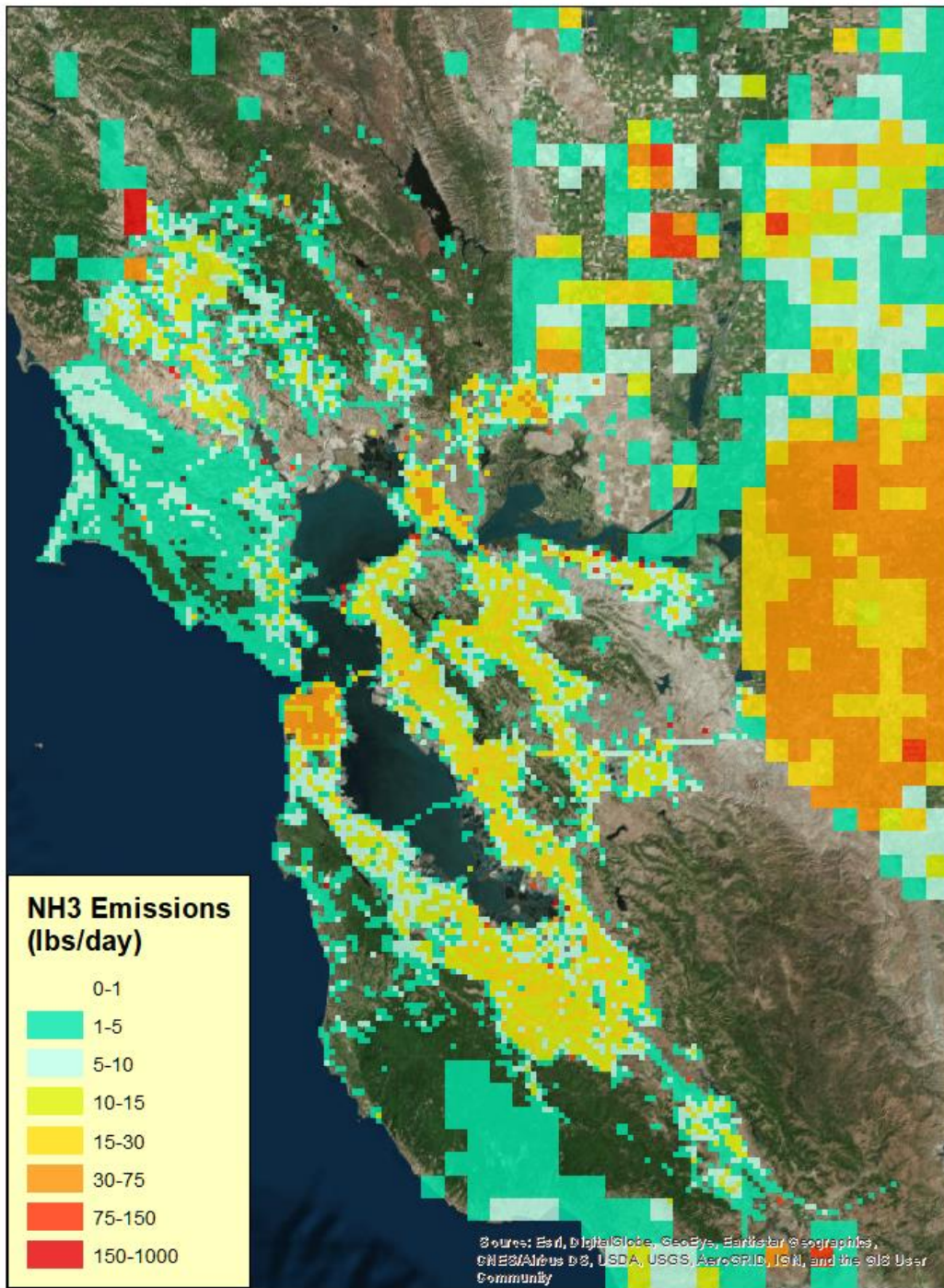


Figure B5: Spatial distribution of annual average NH₃ emissions for the 1-km modeling domain.

APPENDIX C – Meteorological Model Evaluation

C1. Statistical Evaluation

The ENVIRON METSTAT program (Emery et al., 2001) was used to compare the WRF-generated meteorological fields against hourly surface observations archived at NCAR. METSTAT is a statistical analysis software package that calculates and graphically presents statistics such as mean observation, mean simulation, bias error, gross error, and index of agreement.

Hourly time series of observed and simulated surface-layer wind and temperature are presented to evaluate the model performance. Statistics are defined as follows:

Mean observation (M_o): calculated from all sites with valid data within a given analysis region and for a given time period (hourly or daily):

$$M_o = \frac{1}{IJ} \sum_{j=1}^J \sum_{i=1}^I O_j^i$$

where O_j^i is the individual observed quantity at site i and time j , and the summations are over all sites (I) and time periods (J).

Mean prediction (M_p): calculated from simulation results that are interpolated to each observation used to calculate the mean observation (hourly or daily):

$$M_p = \frac{1}{IJ} \sum_{j=1}^J \sum_{i=1}^I P_j^i$$

where P_j^i is the individual simulated quantity at site i and time j . Note that mean observed and simulated winds are vector-averaged (for east-west component u and north-south component v), from which the mean wind speed and mean resultant direction are derived.

Bias error (B): calculated as the mean difference in prediction-observation pairings with valid data within a given analysis region and for a given time period (hourly or daily):

$$B = \frac{1}{IJ} \sum_{j=1}^J \sum_{i=1}^I (P_j^i - O_j^i)$$

Gross Error (E): calculated as the mean *absolute* difference in prediction-observation pairings with valid data within a given analysis region and for a given time period (hourly or daily):

$$E = \frac{1}{IJ} \sum_{j=1}^J \sum_{i=1}^I |P_j^i - O_j^i|$$

Note that the bias and gross error for winds are calculated from the predicted-observed residuals in speed and direction (not from vector components u and v). The direction error for a given prediction-observation pairing is limited to range from 0 to $\pm 180^\circ$.

Root Mean Square Error (RMSE): calculated as the square root of the mean squared difference in prediction-observation pairings with valid data within a given analysis region and for a given time period (hourly or daily):

$$RMSE = \left[\frac{1}{IJ} \sum_{j=1}^J \sum_{i=1}^I (P_j^i - O_j^i)^2 \right]^{1/2}$$

The RMSE, as with the gross error, is a good overall measure of model performance.

Index of Agreement (IOA): calculated following the approach of Willmont (1981). This metric condenses all the differences between model estimates and observations within a given analysis region and for a given time period (hourly and daily) into one statistical quantity. It is the ratio of the total RMSE to the sum of two differences – between each prediction and the observed mean, and each observation and the observed mean:

$$IOA = 1 - \left[\frac{IJ \cdot RMSE^2}{\sum_{j=1}^J \sum_{i=1}^I |P_j^i - M_o| + |O_j^i - M_o|} \right]$$

Viewed from another perspective, the index of agreement is a measure of the match between the departure of each prediction from the observed mean and the departure of each observation from the observed mean. Thus, the correspondence between predicted and observed values across the domain at a given time may be quantified in a single metric and displayed as a time series. The index of agreement has a theoretical range of 0 to 1, the latter score suggesting perfect agreement.

C2. Time Series Comparisons

To further evaluate model performance and to understand the meteorology at specific regions of concern, the simulated results were compared to wind and temperature measurements from monitoring sites in West Oakland, San Jose and Vallejo. Figures C2 through C9 show time series comparing daily average WRF-simulated surface wind speed and temperature to observations at Oakland, San Jose and Vallejo for each quarter of 2016.

The WRF-simulated wind and temperature matched the observed trends very well for the whole year of 2016. There were no significant differences between the predicted and the observed values. The best performance was observed at Vallejo site, especially for wind speed performance. Underestimations of wind speed were noticeable at Oakland and San Jose

throughout 2016. Investigations into this wind speed performance problem are on-going.

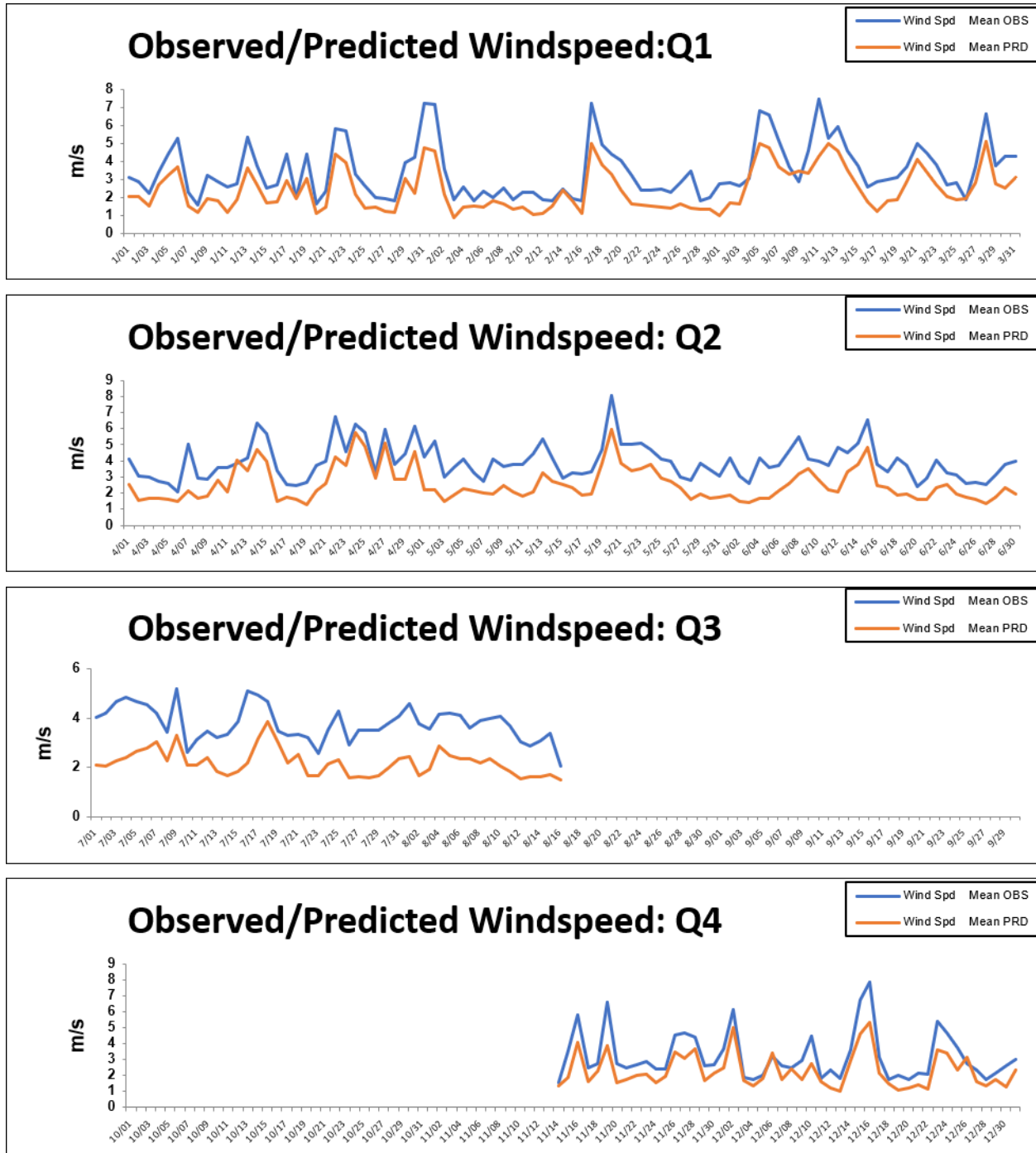


Figure C1: Daily time series of observed and simulated wind speed at West Oakland for 2016 are displayed quarterly. Observation data from mid-August through mid-November were not available. “Mean OBS” is for all observations averaged over the 1-km domain. “Mean PRD” is for all prediction fields at the observation sites averaged over the 1-km domain.

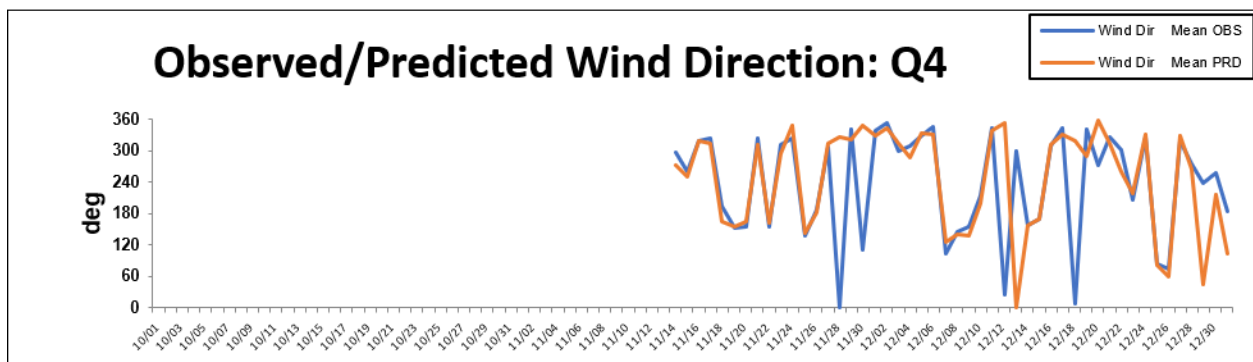
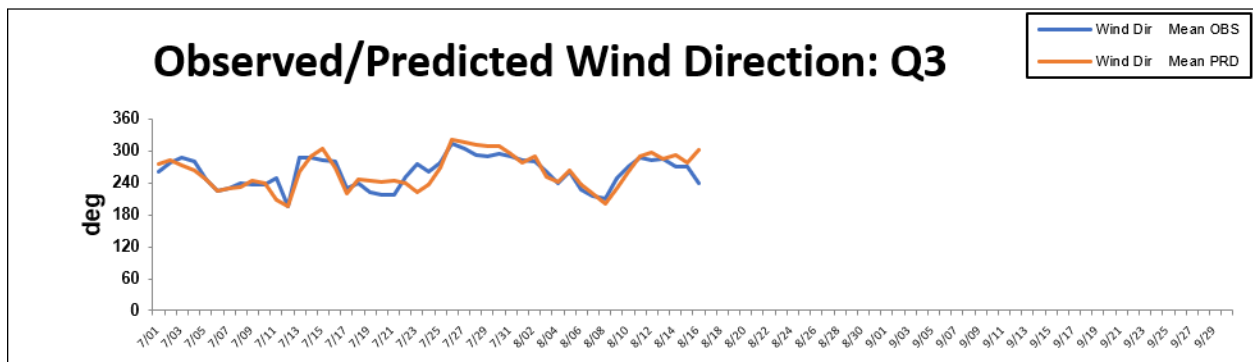
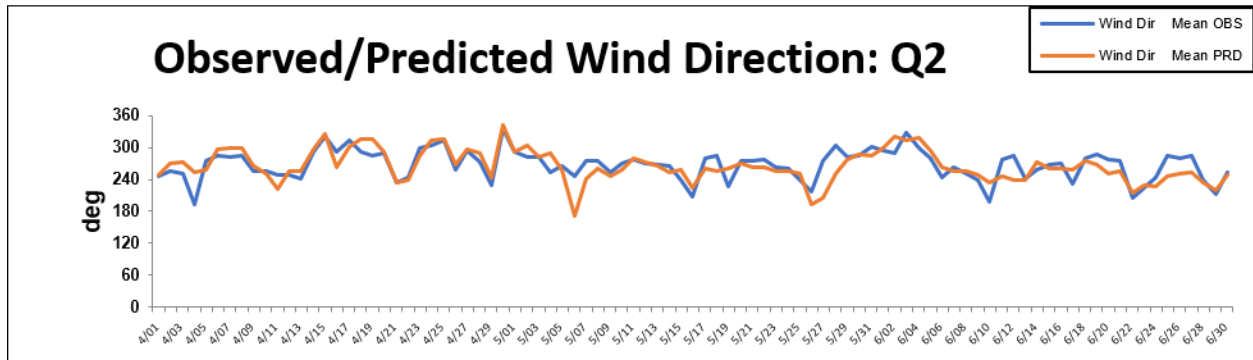
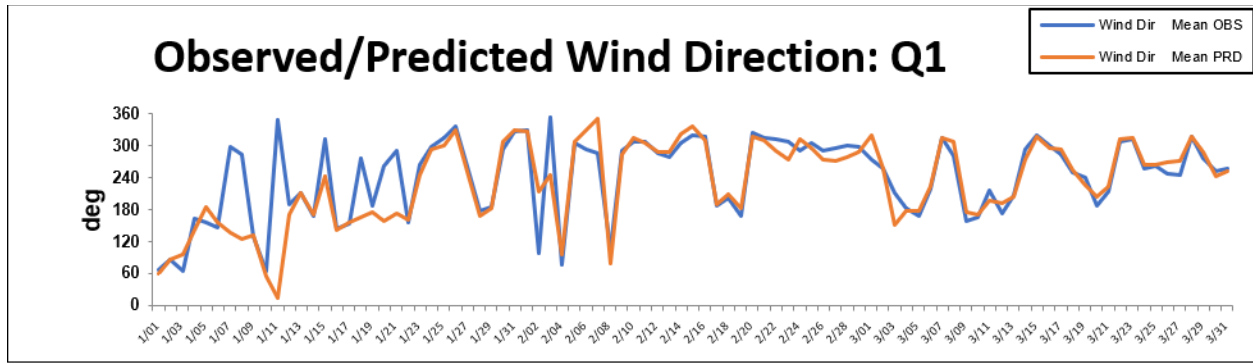


Figure C2: Daily time series of observed and simulated wind direction at West Oakland for 2016.